HURRICANE IRMA IMPACT AND POST-STORM BEACH MORPHOLOGY EVOLUTION IN BOCA RATON, FL

by

Richard M. Hart III

A Thesis Submitted to the Faculty of

Charles E. Schmidt College of Science

In Partial Fulfilment of the Requirements for the Degree of

Master of Science

Florida Atlantic University

Boca Raton, FL

May 2019

HURRICANE IRMA IMPACT AND POST-STORM BEACH MORPHOLOGY EVOLUTION IN BOCA RATON, FL

by

Richard M. Hart III

This thesis was prepared under the direction of the candidate's thesis advisor, Dr. Tiffany Roberts Briggs, Department of Geosciences, and has been approved by the members of the supervisory committee. It was submitted to the faculty of the Charles E. Schmidt College of Science and was accepted in partial fulfillment of the requirements for the degree of Master of Science.

SUPERVISORY COMMITTEE:

Tiffany Roberts Briggs, Ph.D.
Thesis Advisor

Anton Oleinik, Ph.D.

Caiyun Zhang, Ph.D.

Zhixiao Xie, Ph.D.
Chair, Department of Geosciences

Ata Sarajedini, Ph.D.
Dean, Charles E. Schmidt College of Science

Khaled Sobhan, Ph.D.
Interim Dean, Graduate College

4.1.19
Date

ACKNOWLEDGEMENTS

I would like to first and foremost thank my advisor, Dr. Tiffany Roberts Briggs, for her unwavering support, constant encouragement, and guidance during this research, writing, and throughout my entire college career FAU. I also owe a great debt of gratitude to James Gammack-Clark for guiding me in an aspect of this project that will be addressed in further studies. His contributions to my field research were extensive. I would also like to thank my remaining committee members, Dr. Anton Oleinik and Dr. Caiyun Zhang, for their critique and guidance. Furthermore, I would like to acknowledge all of the hard work put in by my fellow students in The Coastal Studies Lab, including but not limited to Joseph Becker, Corey Aitken, Thomas Shahan, Jyothi Palaparthi, Julie Cisneros, Ty Briggs, Nicholas Brown, and Andrew Medhurst. This study required significant time in the field and everyone above was more than happy to go when the call came.

ABSTRACT

Author: Richard M. Hart III

Title: Hurricane Irma Impact and Post-Storm Beach Morphology Evolution in Boca Raton, Fl

Institution: Florida Atlantic University

Thesis Advisor: Dr. Tiffany Roberts Briggs

Degree: Master of Science

Year: 2019

Beach morphology changes naturally with seasonal and event-driven variability in the wave climate, as well as due to anthropogenic activities such as erosion mitigation efforts. In 2017, category four Hurricane Irma caused beach erosion and dune overwash in Boca Raton, FL. Immediate post-storm perigean spring tides coupled with typical winter high-wind conditions imposed a regime of spatially and temporally extended meteorologic and morphologic variability. This study evaluates the morphologic evolution and post-storm recovery in the first year following Hurricane Irma. Time-series topographic surveys and surface sediment samples were collected. Patterns of accretion and erosion were evaluated with regionally measured water and wind levels. Recovery morphology was generally through berm-building, but lacked shoreline stability. Storm impact regime, mitigation structures, and sediment transport patterns drove the recovery. Total volume lost above the 0 m contour due to the storm was not fully recovered within the year, with a large volume measured in the south.

DEDICATION

To my amazing mother, Jane, who has stood by me through the dark and the light, I owe a debt of gratitude I will never be able to fully repay. To my wonderful fiancé, Allison - Not a day goes by I don't thank God you are here to walk through this world with me

HURRICANE IRMA IMPACT AND POST-STORM BEACH MORPHOLOGY EVOLUTION IN BOCA RATON, FL.

LIST OF TABLES

LIST OF FIGURES

INTRODUCTION

Beaches are dynamic environments, changing due to waves, currents, tides, storms, and anthropogenic modifications. Water levels control the spatial extent of the beach under meteorologic influence. Wind drives local wave characteristics, which is another important driver behind the variability of beach morphology. Although South Florida experiences a local reduction in the regional wave energy due to its location within a wave shadow produced by the Bahamas (Benedet, et.al., 2006), its beaches are still subject to periodic erosion from large weather events and seasonal variability. Coastal squeeze further exacerbates erosion, as human-built infrastructure and development creates a hard line with which the beaches ability to respond naturally to sea level rise is diminished (Duran et al., 2016; Pontee, 2013). Florida's beaches have great extrinsic value, as places of recreation and marquee locations to build real estate, as well as providing habitat and serving as buffers against rising sea conditions (whether during storms or long-term sea level rise). Thus, it has long been recognized that a fundamental understanding of the ways in which the beaches respond to varying conditions must be founded in robust monitoring to establish best practices in management. The objectives of this study are to 1) classify the storm-impact regime due to Hurricane Irma, and 2) quantify short-term recovery morphology and rate of recovery (i.e., up to 12 months post-storm). By gaining a greater understanding of the coastal zone in South Florida, and its response to varying conditions, mitigation efforts can be tailored properly, and their

performance can be improved, saving money and providing a more sustainable buffer against further weather events and sea level rise.

The beach is defined by Komar (1998) as "an accumulation of unconsolidated sediment (sand, gravel, cobbles, and boulders) extending from the mean low tide line to some physiographic change" like dunes, permanent vegetation, or anthropogenic structure. As a highly dynamic environment it is constantly under the influence of the sea, the wind, and the meteorologic conditions present at any given time. These conditions include, but are not limited to, tides, storm surge, waves, and longshore currents. Water level and waves are the most consequential influencers of the morphology of the beach. These affecting factors can be separated into two groups, variability based on the seasons and event driven variability. Seasonal changes in the beach are caused by normal changes in the weather, the seasons, and the tides. During the winter, energy in the ocean tends to be greater, with higher waves and wind from the north, southward sediment transport, and some sediment typically transported offshore. During the summer, the energy is less, with smaller waves, sand typically transported onshore, and a reversal in the longshore transport (to the north) (Shahan & Briggs, 2017). When simplifying these seasonal patterns February represents the "seasonally eroded shoreline period" and June/July represents the time when the shore is at its most seaward position (Senechal et al., 2015; Biausque et al., 2016). Elevated tides must also be taken into consideration, as they modulate the water level, allowing wave energy to influence previously unaffected parts of the beach. Multiple times a year the coastal zones are affected by high water events known as perigean spring tides (or king tides), where the moon is at its perigee (or closest proximity) to the earth (NOAA, 2014).

During the summer, the coast can be exposed to the energy generated by large summer cyclonic storms, or hurricanes. These "events" not only produce high waves and winds but can be accompanied by storm surge, with elevated water levels that can reach far beyond those present with extreme tides. In the winter, the large storms generated in the north, called nor'easters (or winter extratropical storms), tend to have a more temporally extended effect (Dolan & Davis, 1991). Wind velocities are less than that of hurricanes, but the erosive effect can be greater as they have a longer duration. Both winter and summer large weather events contribute greatly to sediment removal along the beaches of South Florida. Although tropical storms can induce rapid erosion due to just one event, nor'easters often have a greater influence as they occur more frequently (Benedet et al., 2007). These "extreme events", whether single storms or storm clusters, cause great mobility in nearshore morphology, exhibited in deflation of the beach and scarping of dunes (Scott et al, 2016).

Morphologic variability after a storm is controlled by the impact that the storm has, primarily attributed to the level of the storm surge and wave runup (Sallenger, 2000). One method of determining the impact of a storm, accounting for both the morphology of a barrier island and the meteorologic conditions, is the Sallenger Storm Impact Scale (Sallenger, 2000). The scale is based on the elevation of wave runup in relation to the elevation of either the dune or berm crest (if a dune is absent). The parameters that represents the water level are R_{HIGH} and R_{LOW}, which represent the "high and low elevations of the landward margin of swash relative to a fixed vertical datum". R_{LOW} is the area of the beach that is continually subaqueous. R_{HIGH} is the highest elevation that the water reaches, taking into account tides, storm surge, and wave runup. The regimes

are swash (R_{HIGH} less than base of dune, impact level 1), collision (R_{HIGH} impacting base of dune, impact level 2), overwash (R_{HIGH} above dune, impact level 3), and inundation (dune continuously subaqueous, impact level 4). Each regime assumes a dominant direction of sediment transport, either offshore or onshore, which requires additional validation. Onshore sediment transport is seen commonly in overwash regimes, with sediment being removed from the system in many cases (Scott et al., 2016; Schambach et al., 2018). Schambach et al. (2018) found that relatively low storm surge influenced by lower tide levels prevented the onset of an overwash regime, highlighting the importance of the timing of a storm in relation to the impact scale.

The morphology of the beach immediately after a storm may be drastically altered, and recovery can begin within weeks. After a storm hits, some beaches will go through a cycle with periods of erosion and accretion (Roberts, et. al., 2013; Splinter et al., 2011). Predicted morphology post-storm is that of a deflated beach, with sediment that has been transported offshore (Figure 1). Onshore transport is seen in overwash regimes and alongshore transport and beach rotation along embayed beaches or those with mitigation structures (Scott et al., 2016). In England, during the winter of 2013/2014, strong storm clusters were found to have caused significant erosion of the upper part of the beach, calculated above mean seal level, while sediment was deposited offshore. The distance and depth of this deposition influenced the post-storm recovery process (Scott et al., 2016). Recovery begins immediately after the storm as wave energy dies, with offshore sediment migrating landward and offshore bars becoming welded to the beach, often resulting in a ridge and runnel system (Roberts et al., 2013). Some sub-tidal sediment may not be made available for reconstruction until mobilized by a higher energy

environment like a large winter storm, possibly extending the recovery time into multiple years (Scott et al., 2016). Berm reconstruction and foreshore accretion commonly result in a steep profile as sand deposited just offshore in bars is immediately available to the foreshore. Bar migration tends to take place during the calm conditions following a storm (Brenner et al., 2018; Duran et al., 2016; Maspataud et al., 2009; Roberts et al., 2013; Splinter et al., 2011;), as waves shoal across the bar (Houser et al., 2008, Houser et al., 2015). Tide levels are also known to affect the migration of a bar as the wave break location, whether on the seaward side of the bar (before the crest) or on top of or landward of the crest can vary bar behavior. Landward side wave breaking causes infilling of the runnel and onshore migration with the possibility of erosion of the bar if undertow currents are present, while lower tide levels, with seaward side breaking waves can restrict onshore migration (Houser & Greenwood, 2007).

Analysis of Hurricane Sandy's impact on Fire Island, NY was done on a limited cross-shore area called the Beach Change Envelope (BCE). This is the portion of the profile where the effect of the impact and recovery would be most easily seen on the seasonal and inter-annual scales. Impact and recovery behavior within the BCE at Fire Island post-Sandy showed a landward shift with both narrowing and lowering of the elevation immediately after the storm. Following multiple seasonal nor'easters the profiles exhibited forebeach accretion (with swash bar welding) and widening, with profiles continually widening throughout the summer, and in late summer showing elevation increases in the upper beach. Continual aggradation of the backbeach allowed for dune recovery to take place in subsequent years (Brenner et al., 2018).

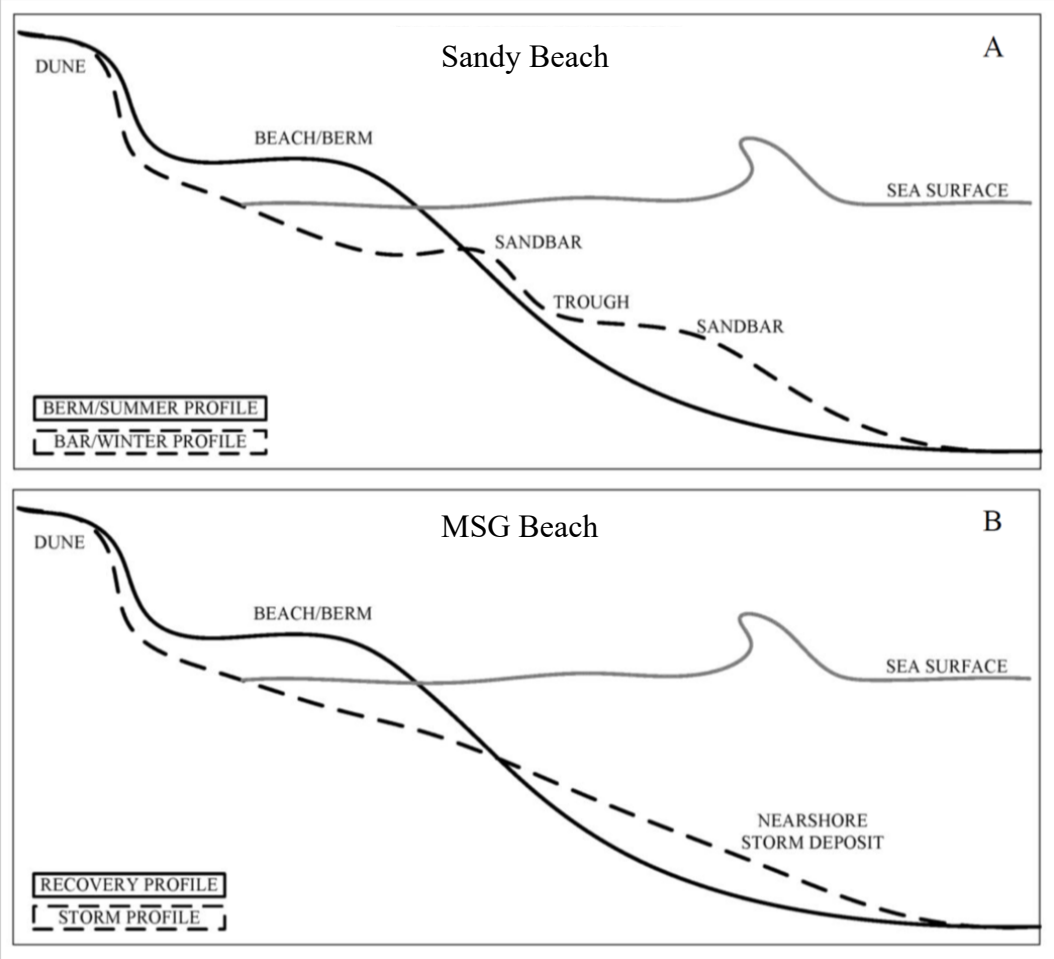

Figure 1. Sandy beach and mixed gravel (MSG) beach conceptual profiles.

The extent of sediment deposition for beach recovery can also be controlled by spring tide water levels (Morton et al., 1994). Water levels can be seen as an aggrading factor in not only the recovery but in the storm impact as well, as sediment is transported onto parts of the beach not regularly influenced by water. During calm conditions swash impacts the foreshore only, creating change. Only during higher energy conditions is the upper beach impacted, making a correlation between shoreline change and overall volume change hard to justify, as aggradation on the backbeach is generally larger and more permanent (Duran et al., 2016). The recovery timescale is variable, based on the

strength of the storm and time between subsequent storms (including winter weather events) (Roberts et al., 2013). The timescale involved in upper beach and dune rebuilding is longer (Splinter et al., 2011), which is consequential as these elevations are factors in the Salleneger Storm Impact Scale, and therefore the primary line of defense against inundation. Temporal and spatial variability in beach morphology also plays a factor in recovery, with closely spaced transects showing possibly different recovery morphologies. Maspataud et al. (2009) found this in Northern France when recovery varied greatly between profiles during fair weather conditions from "noticeable post-storm recovery" to "slight erosion" during their study period.

Timely surveys of the post-storm beach and subsequent months are of great importance for planning and management. Traditionally, one of the most commonly employed methods to measure beach accretion/erosion is by topographic survey (Benedet, et. al., 2006; Browder & Dean, 2000; Coco et. al., 2014; Elko & Wang, 2007; Lee et. al., 2016; Hamm et. al., 2002; Morton et. al., 1994; Roberts & Wang, 2012; Roberts et. al., 2013; Shahan & Briggs, 2017; Elko, 2005). A topographic survey provides information on the physical profile of the beach and enables interpretation of how varying conditions affect morphology. Topographic profiles collected with level, transit, and RTK-GPS has been shown to be more accurate than other methods, with a total accuracy of ± 1cm (Lee et al., 2016).

Monitoring a beach, in consideration to the impact of a hurricane, in a temporally appropriate matter, should include assessment of the topography to quantify volumetric changes and measure the beach slope (Coco et al., 2014). A spatially and temporally comprehensive dataset of time-series beach profiles is often used to quantify changes in

beach volume [e.g., in the Regional Morphology Analysis Package (RMAP)]. Segmenting the beach into sections such as the dry beach, shoreline, and across the entire profile can infer transport direction (Roberts & Wang, 2012). Variability in volume recovered at different cross-shore locations over time suggest that shoreline position alone is not the best metric in measuring recovery or resiliency (Splinter, 2011). Optimally the physical components of a beach monitoring program would be a combination of beach profile surveys and bathymetric mapping combined with the collection of hydrographic and meteorologic data (Browder & Dean, 2000). However, due to equipment, funding, and physical or personnel limitations, measuring all components are not always possible.

Stuable and Kraus (1993) found that using topographic surveys, tied into established monuments with known vertical datum, over long periods of time provided an accurate assessment of a beach's behavior and that by monitoring spatial intervals, based on cross-shore morphologic variability, and increasing them when changes occur, proved to provide a more accurate topological profile. Elko and Wang (2007) found that using topographic surveys to measure Florida's west coast beaches following a busy hurricane season was an effective technique in measuring morphology change. Predicted behavior of a nourishment site following the storm was that extreme erosion would take place, but following a period of continued monitoring the storms actually proved to be a driver to push the coast into an equilibrium state (an equilibrium state being the morphology of the beach is no longer loosing or gaining sediment in a non-cyclical way) (Elko & Wang, 2007). Shahan and Briggs (2017) used similar techniques on Boca Raton's beach to study the performance and evolution of a small nourishment project, finding limitations

on getting full topographic profiles in the subaqueous zone of the beach when the ocean was exhibiting higher energy conditions. These limitations must be considered when surveying in the ocean, as safety of researchers and equipment is paramount.

The efficacy of the use of topographic profile collection on the beach is demonstrated by Ave and Elko (2005) in regard to the active 2004 hurricane season. Beach profile data, along with recorded bathymetry and hydrodynamic conditions, were implemented to monitor the performance of nourishment projects in Pinellas County, Fla. During the scope of that monitoring project Hurricanes Frances, Ivan, and Jeanne impacted Florida. The nourishment performance monitoring dataset, in conjunction with immediate post-storm surveys, provided a comprehensive picture of the impact of the storms. This data was disseminated immediately to the Florida Dept. of Environmental Protection and the US Army Corp of Engineers, resulting in expedited emergency funding for recovery projects. Ba and Senechal (2013) used topographic survey in conjunction with secondary hydrodynamic data provided by offshore buoys to compare the behavior and recovery of a beach to the different conditions of the winter vs. the summer. By combining a robust analysis of tide level, wave height and period, longshore current direction, and topographic profile the authors were able to attribute the predicted accretion and erosion of the beach (during the summer and winter respectively) to specific hydrodynamic conditions.

Changes in beach sediment texture can also provide inferred information about hydrodynamics, transport direction, and recovery. Sediment transport is dependent on variation in the grain size, density, shape, sphericity, and roundness of the grains, with finer grains being sorted out of areas of high energy and transported to areas of less

energy (Meijer, et. al., 2002). Factors which control the mean grain size are the sediment source, the wave energy level, wind, and the offshore slope on which the beach is constructed. Onshore winds can vary distribution in the fine fraction on the beach (Yu et al., 2013), while bottom topography, turbulence, and wave-energy dissipation also play a role in sediment dynamics (Komar, 1998). Post-storm accretion of fine to medium sand in conjunction with profile adjustment was a metric of recovery along Asian beaches following a particularly active typhoon season, with relative stability in grain size being noted in the upper beach and grain size fractions in the lower beach and intertidal area exhibiting greater fluctuation (Yu et al., 2013). Roberts, et. al. (2013) found well sorted medium sand at the surface of the backbeach, likely deposited during the subsidence phase of a large winter storm. Shahan and Briggs (2017) found a coarsening at the -0.5m water depth, attributing it to higher wave energy and onshore transport of fines during the perigean spring tides as deposition took place on the upper portion of the beach. Therefore, sediment distribution along a post-storm profile can be an indicator of impact severity and dynamics of transport during post-storm recovery.

METHODS

Study Area

The study area for this research is located in Boca Raton, Florida and encompasses a section of its beach stretching approximately 2.5 km north of the Boca Raton Inlet (Figure 2). The beach in this part of Florida is morphodynamically classified as intermediate, which encompasses a high degree of morphologic variability (Benedet, et. al., 2006). The beach is relatively straight with hard structures (a jetty, groins, an outcrop, and hard bottom) interspersed throughout. The area is bounded by the Boca Inlet to the south. Boca Raton's coastline is located in an area where the predominant wave energy of the greater Atlantic Ocean is blocked by the Northern Bahamas, therefore it shows a marked difference from areas further north, or even adjacent in northern Palm Beach, Martin, and St. Lucie counties. The areas' geologic bedrock is the limestone of the Anastasia formation. Variability in wind and waves seasonally is a norm in coastal environments, with South Florida showing a wind direction and current trend from the north in the winter and from the south during the summer. Furthermore, extensive erosion and mobility can be traced to the effects of seasonal weather patterns and weather events. These are considered to be nor'easters during the winter, with prolonged heavy surf and wind originating from the north, to hurricanes and tropical storms that occur during the mid to late summer season, showing a variable (i.e. rotational) wind and current direction based on the location of the storm and duration of the impact. Yearly

offshore significant wave heights in Boca Raton average 0.85 m with a period of 6.8 s (NOAA, 2016).

The study area was impacted by Hurricane Irma between September 9th and September 12th, 2017 with the strongest winds of the storm affecting the area at 9 pm the night of the 10th (Figure 3). While Hurricane Irma was a category 4 storm on the Saffir-Simpson scale as it approached the Florida Keys, conditions in Boca Raton were sustained winds of approximately 63 mph with gusts up to 90 mph . The highest water levels were seen in the late afternoon of the 10th, with levels approaching 0.5 m above predicted tide levels. Water levels subsided quickly and were back to predicted levels by 6pm on the 11th, while the wind speed stayed elevated throughout the night and into the 12th (NOAA, 2019). Maximum and mean water levels for the entire study period are shown in figure 4 and wind conditions for the study period are shown in figure 5.

A. Distances Between Profiles

R215 – R215A	400 m
R215A – R216	500 m
R216 – R217	375 m
R217 – R217A	315 m
R217A – R218A	325 m
R218A – R219A	215 m
R219 – R220	315 m
R220 – R221	265 m
R221 – R222	285 m
R222 – R223	325 m

B. Profiles with structural influence

R215	Directly north of a groin
R215A	Directly south of groin with hard bottom
R219	North of limestone outcrop
R220	South of limestone outcrop
R221	North of groin
R222	South of groin
R223	Directly north of jetty for Boca Inlet

Table 1. Distances between profiles (A) and Profiles with structural influence (B)

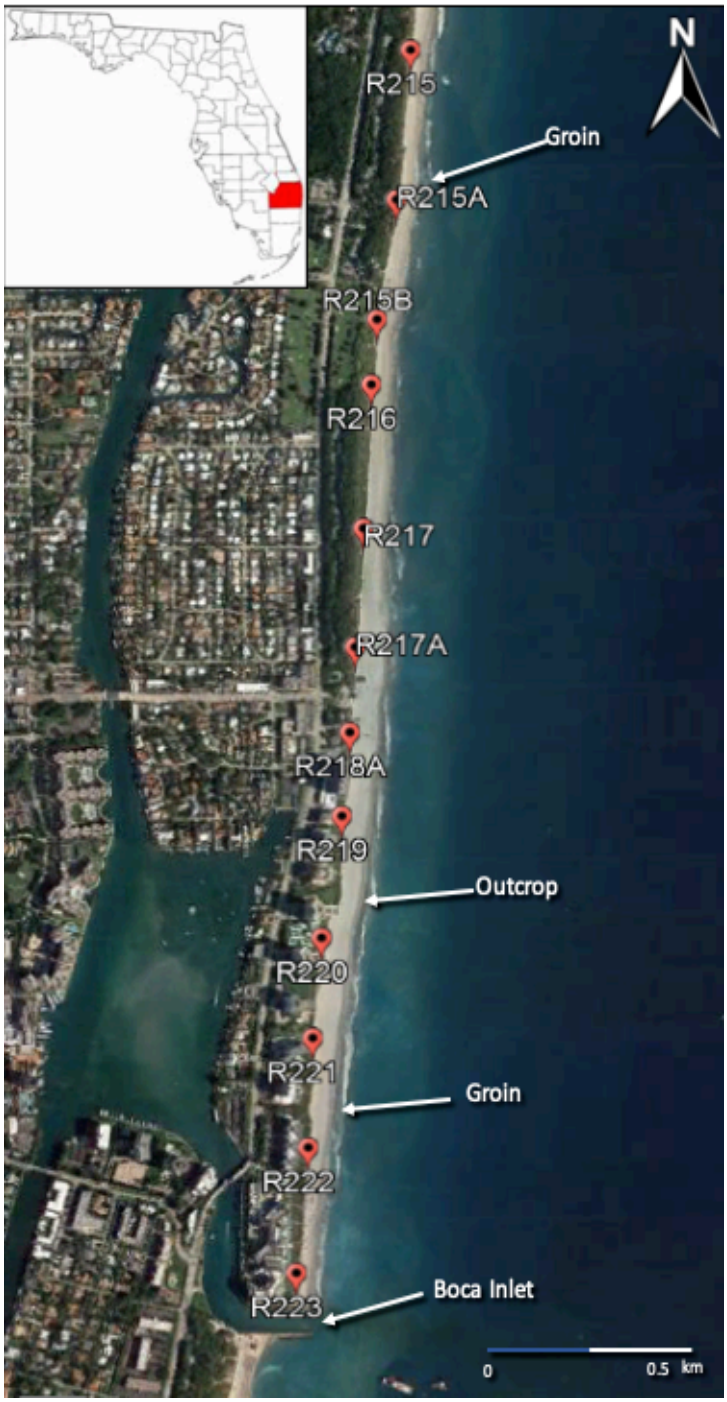

Figure 2. Study Area – Pins represent monuments set for survey transects included in the study and features with potential influence are noted in orange (Map data: Google, DigitalGlobe).

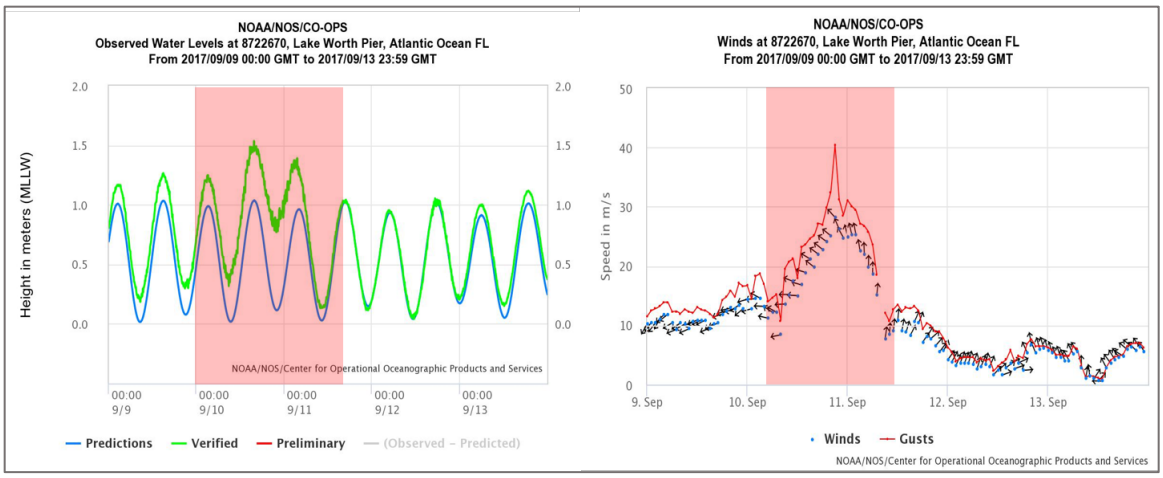

Figure 3. NOAA Tides and Currents water level readings at station 8722670 for Sept. 9 to Sept. 13. With Hurricane Irma water levels and wind speeds are indicated with bounded areas representing the period of highest impact (NOAA, 2019)

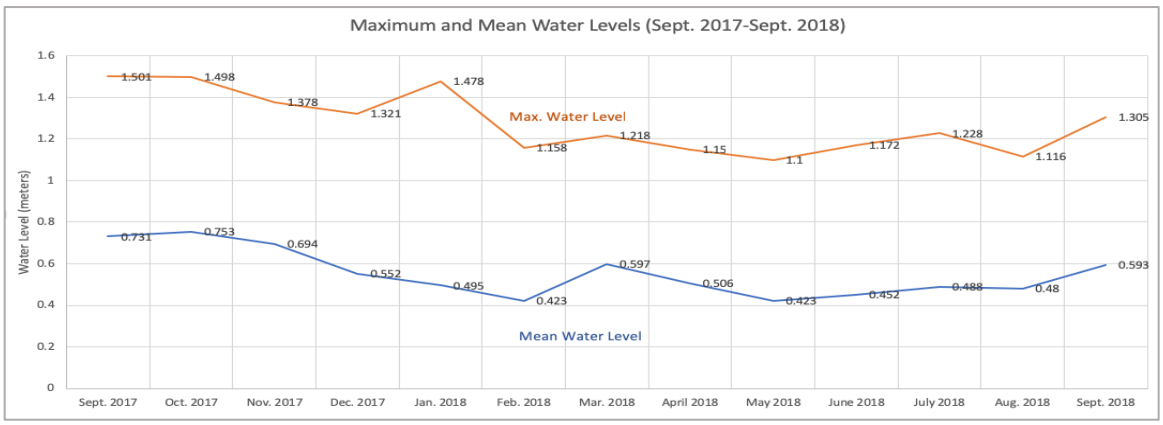

Figure 4. Maximum and Mean Water Levels (Sept. 2017 – Sept. 2018)

Figure 5. Maximum sustained winds for (A) 2017 and (B) 2018. Highlighted areas represent sustained winds in excess of 15 m/s (33.5 mph) and are considered high wind events for this study. Yellow lines demarcate the start and end of the study period.

Beach Profiles

Topographic profiles were created by collecting data along 10 transects over a period of one year with a Trimble TS635 total station and 8 ft. survey rod. Points were shot from the dune toe to approximately -3 m water depth (depending on ocean conditions). Control points for the transects were set with a Real Time Kinetic Global Positioning System (RTK GPS) and established by the Coastal Studies Lab at FAU. These control points were named based on their vicinity to R-monuments established by the State of Florida, which are spaced approximately 300 m apart. Spatial resolution of the points taken during surveys was based on the variations in the morphology at the beach at the time of data collection (e.g., to ensure detailed mapping where slope changes

were evident). Survey data was collected on a monthly basis with temporal resolution being increased in response to weather events (i.e. pre-and post-storm data collection to capture the immediate impact on morphology).

Sediment Sampling

Sediment samples, collected at three cross-shore locations, were taken from the upper ~10 cm of sand, with an average sample size of ~200 g. Samples were collected on the same day as the surveys and labeled to represent which transect that they came from. Cross-shore samples were collected at the shoreline (~0m NAVD88), the mid-beach (delineated in the field by approximately halfway between the monument and the shoreline in an area of flat morphology), and the dune toe [the area at the base of the dune that would interact with water in a collision regime (Sallenger, 2000)]. Sediment grain sizes are described in phi (Φ) units and based on the Wentworth scale (Wentworth, 1922). Coarse sand is 1 – 0 phi (0.5 – 1 mm), medium sand is 2 -1 phi (0.25 – 0.5 mm), and fine sand is 3 – 2 phi (0.125 – 0.250 mm). Sorting is based on the standard deviation (σ) of the sediment samples statistics. Very well sorted (under 0.35 Φ σ), well sorted (0.35 – 0.50 Φ σ), moderately well sorted (0.50 – 0.71 Φ σ), moderately sorted (0.71 – 1.0 Φ σ), poorly sorted (1.0 – 2.0 Φ σ), and very poorly sorted (2.0 – 4.0 Φ σ) are the sorting classifications used in this study.

Water Level and Wind Information

Water level (tide) and wind data was acquired through NOAA's Tides and Currents program, from station 8722670, located at the Lake Worth, Fl. pier (lat. 26.60,

long. 80.03). Water levels, or surge, was analyzed in relation to the level above predicted values. Wind speed and direction is considered as it is a driver for local wave conditions, in which data was not available.

Data Analysis

Topographic point data was downloaded from the field collector and presented as a northing, easting, elevation, and distance. Monument elevations are variable due to the being lost in storms, etc. and are reset with an RTK GPS system. Elevation data was plotted to create topographic profiles representing the physical shape of the beach, and analysis of these profiles was done to quantify cross and along shore variability. Easting, northing, elevation, and distance tables (X, Y, Z, d) were imported into the Regional Morphology Analysis Package (RMAP), developed by the U.S. Army Corp. of Engineers, to analyze the volume of the beach at different cross-shore elevations (the dry beach being volume being calculated above 1 m elevation and the shoreline being calculated above 0 m elevation). Sediment samples collected were washed and dried for approximately 5 days. The sediment texture was determined using a mechanical Ro-Tap at quarter phi intervals between -4 phi to +4 phi (16 mm to 62.5 μm). Granulometric statistics were calculated using the moment method to determine mean, standard deviation (sorting), skewness, and kurtosis (in phi and mm), allowing more in-depth morphologic analysis of the processes influencing the beach to taken.

RESULTS

Results are presented as overall morphology change with respect to time (months) throughout the study, followed by volume change analysis of the study area, followed by sediment analysis of sand gathered at critical sampling sites during the study. Pre-Irma data was collected in late July and August of 2017. The pre-Irma data represents a baseline for this study and the subsequent impact and recovery that occurred. A nourishment project was completed in the study area between 2016 – 2017, encompassing R217 in 2016 and R217A – R223 in 2017.

Morphology over time

Hurricane Irma Impact (Aug. 2017 – Sept. 2017)

Hurricane Irma impacted the study area between Sept. 9th and Sept. 12th with sustained winds of approximately 63 mph and surge 0.5 m above predicted values. Profile surveys completed the previous month, in Aug. 2017 are used for pre-storm conditions and are the baseline for storm-recovery. All profiles with the exception of R223 (jetty adjacent) exhibited similar erosion and retreat patterns, with variability in the severity immediately after the storm. Shoreline retreat ranged from 5 m at R222 to 15 m at R220, with average shoreline retreat of the being 11.3 m. The beachface retreated an average of 12 m on the profiles and there was marked retreat on the dry beach. Most profiles gained backbeach elevation with only R215A exhibiting deflation, losing 0.25 – 0.5 m of elevation, and R223 showing little to no change. All profiles with exception of R215A had marked deposition in the nearshore at around -1 m elevation, which is

indicative of storm induced beach erosion (Figure 6). Impact regimes based on the Sallenger Storm Impact Scale varied between swash, collision and overwash throughout the area. R218A, R221, and R223 experienced a swash regime, with little impact in the dune area while R215, R215A, R217A, R220, R221, and R222 experienced collision. An overwash regime occurred at R216 and R217, with significant backbeach deposition beyond the dune. Pre and post-Irma profiles at selected locations with impact regime indicators are shown below (Figure 6).

Immediate Recovery Period (Sept. 2017 – Oct. 2017)

Surveys completed a month after the impact showed overall accretive recovery with some outliers. R215 (north of a groin) showed very little change while R215A showed 8 m retreat in both the shoreline and the beachface. R216, R217 (Figure 7A), R217A, and R218A (Figure 7B) all showed profile inflation above 1 m contour with shoreline advance or stability. All of these locations exhibited berm building 40 m from the monument with inflation between the 1 and 2 m elevation contours. R220 (south of outcrop) retreated 5 – 7 m overall. Inflation of the dry beach above the 1 m elevation contour occurred at R221 and R222, with R221 remaining otherwise stable. At R222 (south of groin) the beachface and shoreline retreated. R223 saw minor deflation in the backbeach but significant advance and accretion across the remainder of the profile, with a shoreline and beachface advance of 15 m.

Swash Regime

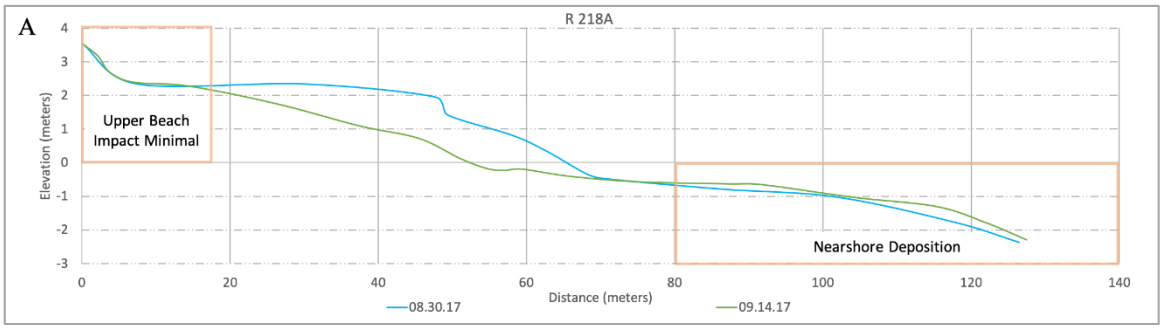

Collision Regime

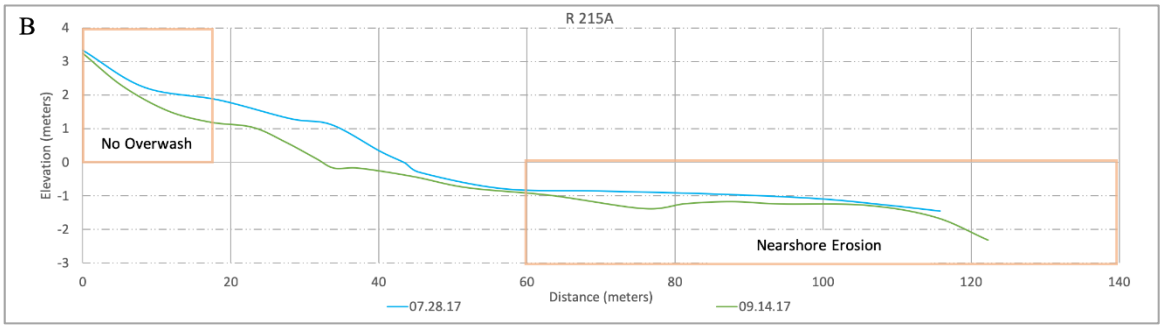

Overwash Regime

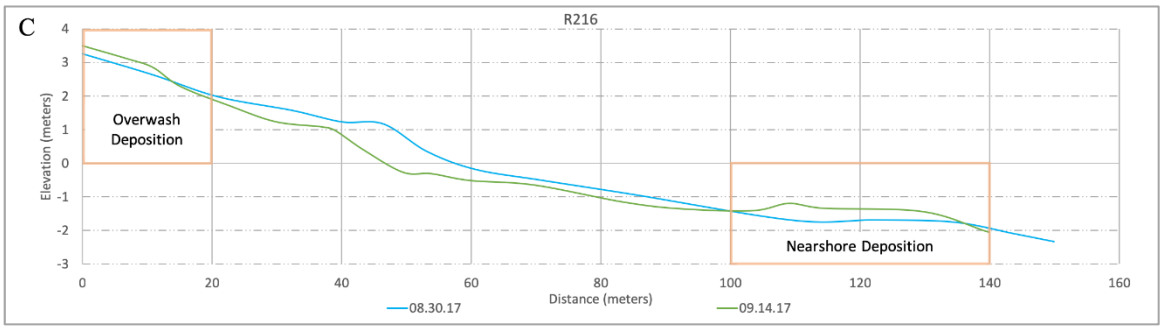

Figure 6. Pre and Post-Irma profiles at (A) R218A, (B) R215A, and (C) R221 with deposition patterns indicative of storm impact highlighted.

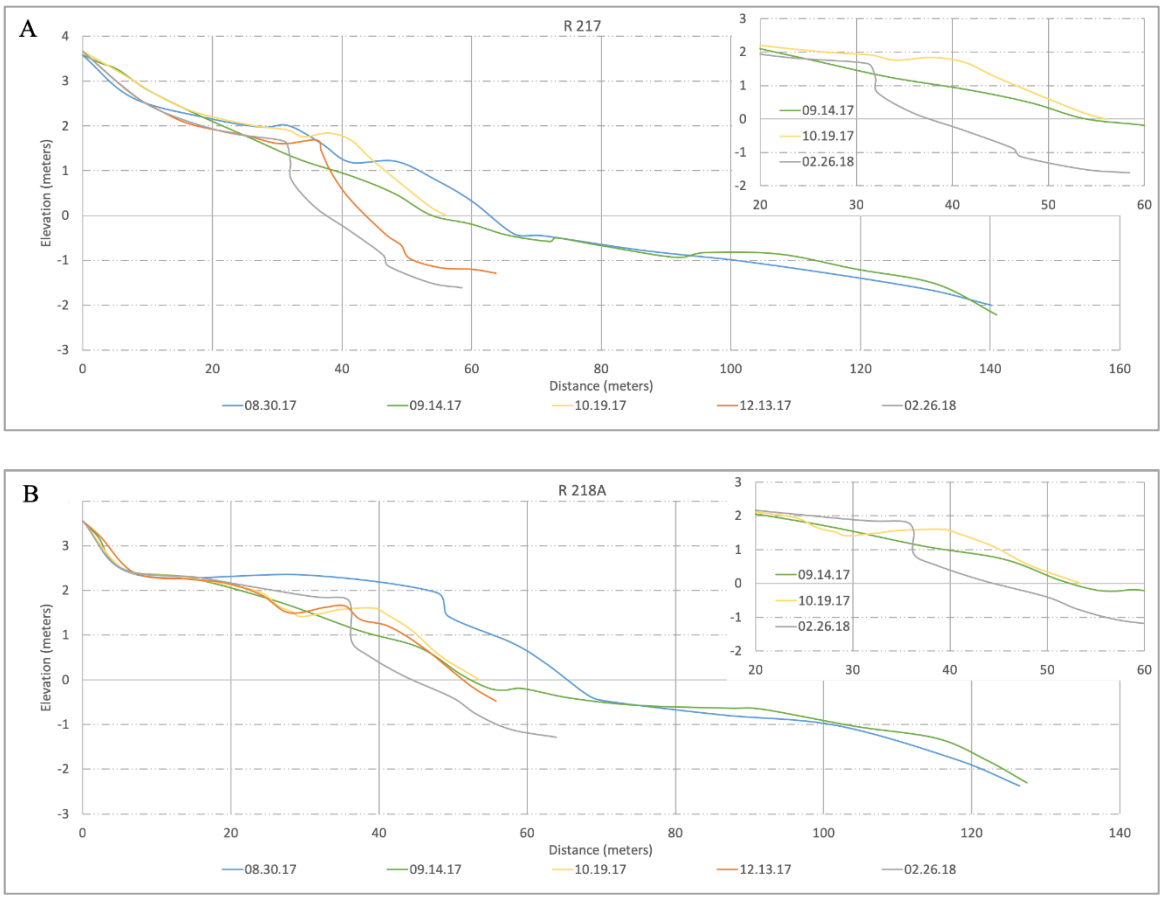

Figure 7. Profiles of (A) R217 and (B) R218A from Aug. 2017 to Feb. 2018 showing similar patterns of deflation and retreat (post Irma), dry beach accretion (Oct.), late fall retreat (Dec.), and winter erosion and scarp formation. Insets on top right highlight morphologic similarities between the two profiles with the pattern measured at R216 and R217A also.

Fall of 2017 (Oct. – Dec.)

The overall trend seen during this period was that of deflation, erosion, and retreat in the north of the study area and inflation, accretion, and advance in the south. Sediment redistribution took place at R215A (Figure 8A), with deposition above 2.5 m elevation, erosion above 1.75 m elevation, deposition and advance above 0.25 m elevation, and shoreline erosion. This is a pattern seen throughout the study to various degrees, and as a pattern was present at R222 during this time period, which is directly south of a groin (Figure 8B). R216 and R217 showed retreat of the beachface and shoreline between 8

and 12 m. Declining losses were measured moving south to R217A and R218A, with retreat of approximately 6 m and 3 m respectively. South of the outcrop profile advance of 6.5 m occurred at R220 and 4 m at R221. R222 showed cross shore sediment distribution (Figure 8B) while R223 showed profile advance of 3 m.

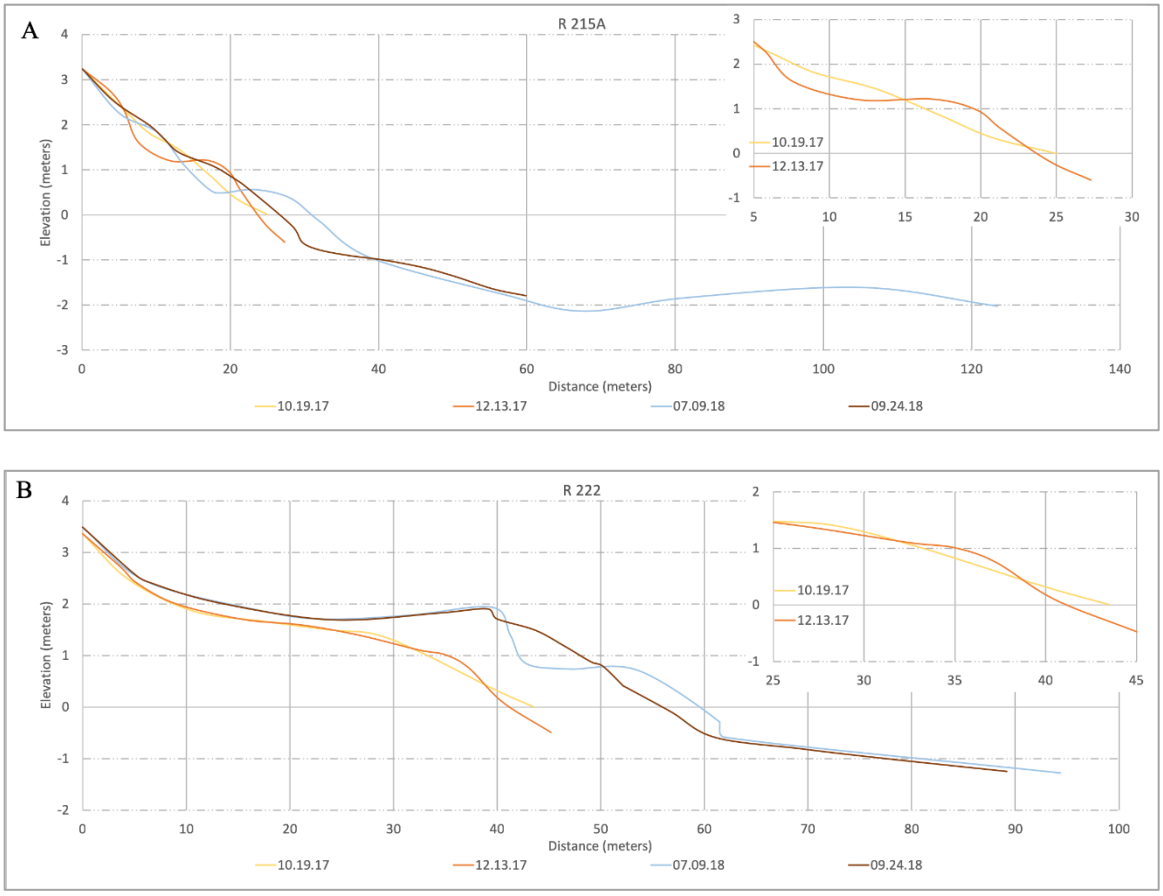

Figure 8. Cross shore sediment redistribution exhibited in profiles (A) R215A and (B) R222, each of which is directly south of a groin, during the fall of 2017 and the late summer of 2018. Insets highlight similar behaviors of erosion above 1 m elevation and deposition below with no shoreline retreat.

Early Winter 2017/2018 (Dec. 2017 – Jan. 2018)

Due to weather considerations profile data was collected only for R216, R217A, and R218A during this period. R216 advanced 8 m in the shoreline and 3 m in the

beachface, with flattening of a berm that was present above 1.5 m elevation, indicative of cross shore sediment redistribution. R217A retreated 5 m overall with a small 0.3 m scarp forming above 1 m elevation. R218A, while showing overall shoreline and beachface retreat, inflated slightly above 1.25 m elevation.

Mid-Winter 2018 (Dec. 2017 - Feb. 2018)

Morphologies present within the study area during this period were highly variable. In the north, profiles R215, R215A, and R216 all saw advance, slight in the very north at R215 and R215A and quite significant at R216, with beach face and shoreline advance of 10 m. R217 exhibited profile retreat of 6 – 7 m, scarp formation between 1 and 2 m elevation, and no change above 2 m elevation. A small scarp that had formed and was flattened at R217A, while R218A retreated 3 – 4 m and formed a similar scarp to R217. R220 saw loss across the entire profile, retreating 7 – 9 m, while R221 (north of groin), saw advance across the profile, with the shoreline advancing 10 m. R222 saw similar profile advance in the beach face and shoreline but in the form of a steep scarp. All profiles except for R223 showed little to no change in the back beach and dry beach. R223 had a 1 m inflation of the dry beach above 2 m elevation with beach face and shoreline retreat of 4 m.

Late Winter 2018 (Feb. – Mar.)

This period was marked by cross shore variability and few north – south trends. While R215 saw advance and inflation, gaining 0.5 m elevation along the entire profile, R215A only inflated above 1.5 m elevation, forming a berm. Between 1.5 and 0 m elevation the profile deflated and below the shoreline it began to advance, indicative of cross-shore transport. R216 showed the same shape as R215A but with double the linear

advance, primarily a function of beach width. R217 showed a similar pattern also, with an inflation above 1.5 m elevation and erosion below, flattening the scarp present in mid-winter (Figure 7A). R217A advances overall, as does R218A, which advances beyond the scarp present in mid-winter (Figure 7B). R221 inflated above 2 m elevation, retreated 3 m at the beach face and retreated 7 m at the shoreline. R222 inflated 1 m above 1 m elevation, reducing a scarp present from mid-winter, and advanced at the beach face and the shoreline by 2 – 3 m. R223 deflated above 2.5 m elevation by 1 m and the beach face and shoreline advanced 2 m. The profiles with alternating deflation / inflation, advance / retreat show morphologic behavior similar to the examples shown in the Figure 8 insets.

Early Spring 2018 (Mar. – May)

Variability in timing of some surveys in the spring and the summer is due to equipment and weather considerations. Some profiles were surveyed in March and April, while others skipped April. There was no change in the morphology at R215 and R215A showed cross shore variability, with deposition occurring above 2 m elevation, while below retreated 8 m. R216 flattened slightly and retreated 3 – 4 m along the beach face and shoreline. The remaining profiles showed consistent advance, ranging from 2 – 5 m at R217 and R217A to a maximum of 7 – 8 m at R220. The south of the study area showed 3 – 5 m advance while the southernmost line, R223, showed variability in the upper beach and no change along the beach face and shoreline.

Mid-Spring (April – May)

Surveys were done at R215, R217, R217A, and R218A encompassing this period. No notable change was measured at R215 for the second survey in a row. R217's profile

advanced slightly (1 m), while R217A showed retreat at the shoreline and nearshore. R218A showed no notable change for the second survey in a row.

Late Spring (May – June)

Overall this period was a period of advance, but with some significant cross shore variability (Figure 9). R215 (Figure 9A) showed a deflation of the profile between 0.5 and 1.5 m elevation, creating a ridge, with 1 – 2 m of sediment accretion and advance on the shoreline and nearshore. At R215A a berm deflated between 1.2 and 2.2 m elevation and the beachface and shoreline advanced 8 – 9 m, forming a ridge and runnel, evidence of cross-shore sediment movement. At R216 (Figure 9B) a 5 m retreat above 0.5 m elevation occurred, with a 10 m advance of the beach face, shoreline and nearshore with a ridge and runnel formation appearing. This same pattern appears moving south down the beach with less severity. Although R217 had little change it shows the sinusoidal pattern shown in Figure 8. R217A exhibits the same pattern with 2 m retreat at 1 m elevation and 2 – 3 m advance at the beachface and shoreline. R218A (Figure 9C) showed the same pattern with even more variability as a berm formed between 1 m and 2 m elevation. R220 and R22l continued with the same sinusoidal morphology, but with little change. R222 (Figure 9D) deflated and retreated 5 – 6 m between 0.5 and 1.8 m elevation with beachface and shoreline advance of 2 – 3 m. The morphology that appeared is very similar to R216 during this time period, although the shoreline / nearshore advance is significantly less. Deflation above 2.2 m elevation and beachface and shoreline retreat of 5 m occured at R223.

Early Summer 2018 (June – July)

During this period profiles in the north showed either no substantial change or slight advance. R215 showed flattening of the scarp that had formed in June. At R215A the berm that had been transitioning downward since May levels off with a deflation of 0.5 m above 0.5 m elevation and shoreline advance of 3 m. R217 gained 3 m of beachface, shoreline, and nearshore, while R217A retreated slightly. R218A showed little change while R221's beachface and shoreline retreated 3 m. R221 and R222 showed slight overall inflation with little change occurring at R223.

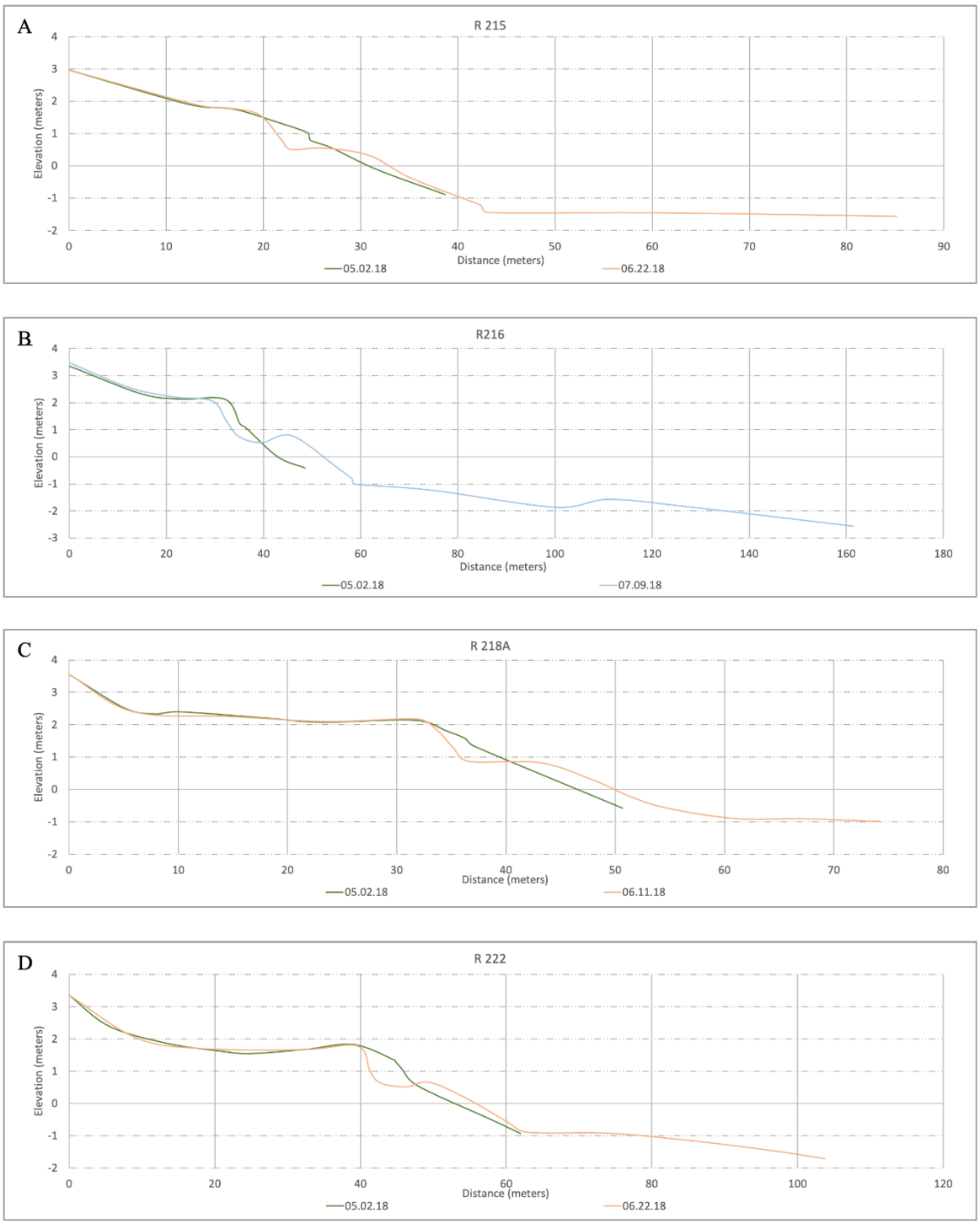

Figure 9. Late spring / early summer profiles of (A) R215, (B) R216, (C) R218A, and (D) R222 exhibiting similar morphodynamic in late spring, evidence of cross shore sediment transport. This pattern was also measured at R215A and R217A.

Late Summer 2018 (July – Sept.)

During the late summer cross-shore variability, again, became prevalent in the study area. 3 m of beachface, shoreline, and nearshore retreat took place at R215. The ridge that had been moving down at R215A disappeared and the profile flattened, advancing 5 m above the flattened July berm and retreating below. R216 inflated 1 m between 0.6 and 1.8 m creating a new ridge and runnel formation at 1.5 m elevation. This section of the beach advanced by 10 m with retreat of 2 m at the beachface, shoreline, and nearshore. There was deposition outwards of the nearshore with nearly 1 m of sediment accreting between -2 and -1 m elevation. Advance of 8 m was measured between 0.5 and 1.5 m elevation at R217 with accompanying shoreline and nearshore advance of 2 – 3 m. The only change at R217A was accretion at the nearshore between -1 and -2 m elevation. R218A showed an inflation above 1 m elevation and deflation below, flattening out the sinusoidal pattern of the profile with 4 m retreat of beachface and shoreline. Retreat of 3 m below 2 m elevation to the shoreline occurred at R220, with deposition below -0.5 m elevation. R221 inflated 0.3 m above 1.5 m elevation while deflating below, resulting in beachface and shoreline retreat of 5 m, while nearshore deposition occurred at -1 m elevation. An inflation above 0.8 m elevation and deflation below flattened out R222, altering the shape that had been present since June (Figure 9D). Deflation of the berm above 1.2 m elevation at R223 caused a retreat of the dry beach by 4 m while the upper beach and shoreline remained stable

.

Volume Change Analysis

Hurricane Irma Impact (Aug. 2017 –Sept. 2017)(Figure 10)

All profiles across the study area experienced sediment loss at both elevation contours (above 0 m for shoreline and above 1 m for dry beach) with the exception of R215, the northernmost profile, which experience negligible volume gain (0.6 m^3/m) in the dry beach coupled with loss at the shoreline of 11 m^3/m. R215A, located directly south of the groin, lost 18 m^3/m of dry beach and 30 m^3/m of shoreline. The most significant losses were measured at R217A and R218A which are in the middle of the study area and located north of the outcrop. These profiles lost nearly equivalent volumes at each elevation contour (41 m^3/m^3 at the shoreline and 21 m^3/m). R223 was the only profile that showed a greater amount of dry beach loss (7 m^3/m) than shoreline (2 m^3/m), which was the lowest amount of shoreline loss measured post-Irma. Average volume loss at the dry beach in the north (R215 – R216) of the study area was 7 m^3/m, over the center section (R217-R218A) was 20 m^3/m, and in the southern section (R220 – R223) was 11 m^3/m. Average shoreline volume losses were 18, 32, and 17 m^3/m at the north, central, and southern section of the study area, respectively.

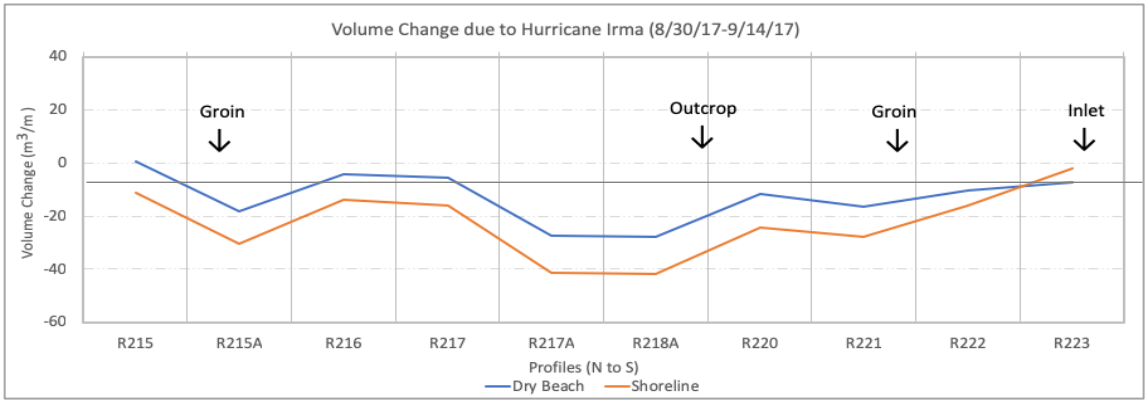

Figure 10. Hurricane Irma impact volumetric change at the dry beach (+1m NAVD88) and the shoreline (0 m NAVD88). The location of structures within the study area is indicated.

Hurricane Irma Immediate Recovery (Sept. 2017 – Oct. 2017)

Within a month of Irma volume had increased overall, with all profiles accreting to varying degrees with the exception of R215 (showing a loss of 1 m^3/m at the shoreline), R215A, and R220, which each lost around 1 m^3/m at the dry beach and 8 – 9 m^3/m at the shoreline. R217A and R218A responded similarly with 2 – 5 m^3/m gain at the dry beach and 3 – 6 m^3/m at the shoreline, repeating a pattern of comparable response from the Irma impact time period. The most significant recovery volume was measured at R223, which is jetty adjacent, gaining 22 m^3/m of sediment at the dry beach and 38 m^3/m at the shoreline elevation (Figure 11). Average volume change at the dry beach in the north (R215 – R216) of the study area was negligible, over the center section (R217-R218A) was 6 m^3/m, and in the southern section (R220 – R223) was 8 m^3/m. Average shoreline volume change was -1, 8, and 10 m^3/m at the north, central, and southern section of the study area, respectively.

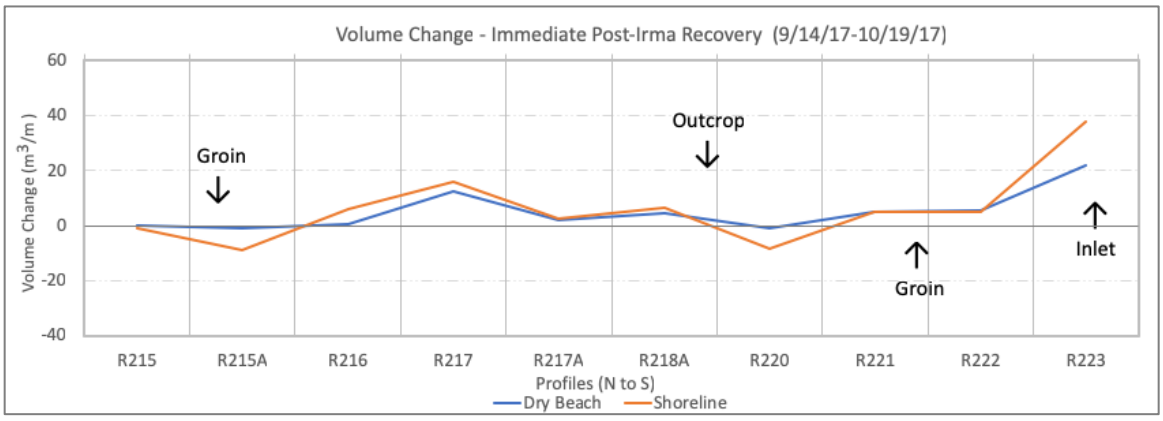

Figure 11. Immediate recovery volumetric change at the dry beach (+1m NAVD88) and the shoreline (0 m NAVD88). The locations of structure within the study area is indicated.

Winter High Energy Period (Oct. 2017 – Feb. 2018)

The study area's response during this period, encompassing perigean spring tide events and early winter high energy events was highly varied. Average volume change at the dry beach in the north (R215 – R216) of the study area was 1 m^3/m, over the center section (R217-R218A) was -6 m^3/m, and in the southern section (R220 – R223) was 11 m^3/m. Average shoreline volume change was 2, -17, and 11 m^3/m at the north, central, and southern section of the study area, respectively. The northern 3 profiles (R215, R21A, and R216) had similar responses gaining between 0.5 and 2 m^3/m at the dry beach and 2 – 6 m^3/m^3 at the shoreline. R217 had the greatest volume loss during this period, loosing 17 m^3/m at the dry beach and 34 m^3/m at the shoreline, with decreasing losses occurring southward. The southern end of the study area (R221, R222, and R223) gained volume at both the dry beach and shoreline. R221 and R223, both just north of structures gained 9 and 22 m^3/m at the dry beach, respectively, and 20 m^3/m at the shoreline.

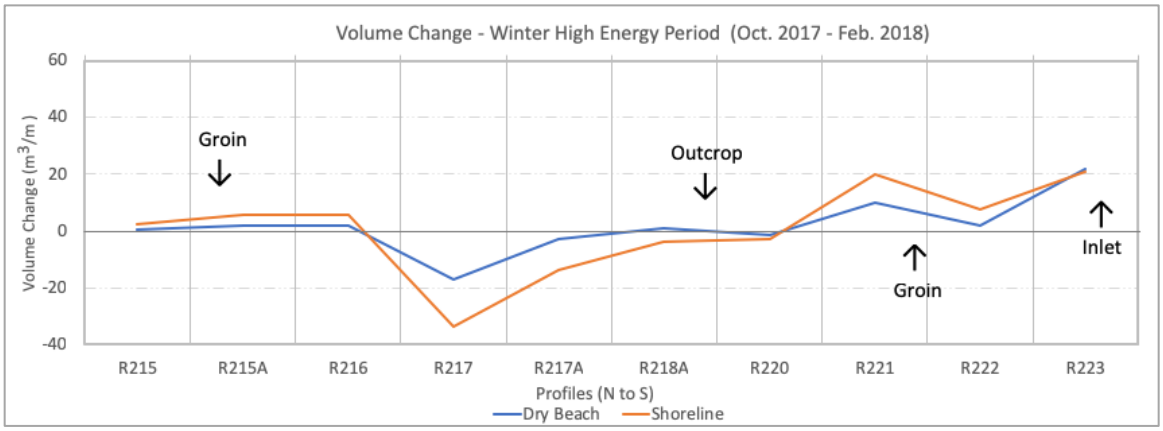

Figure 12. Volumetric change at the dry beach (+1m NAVD88) and the shoreline (0 m NAVD88) between Oct. 2017 and Feb. 2018. The locations of structures within the study area is indicated.

Summer Low Energy Period (May 2018 – Sept. 2018)

The period between May and September, a time of typically lower energy (barring the occurrence of tropical disturbances), had the least variability in volume during the study (Figure 13). Average volume change at the dry beach in the north (R215 – R216) of the study area was 1 m^3/m, over the center section (R217-R218A) was 6 m^3/m, and in the southern section (R220 – R223) was -2 m^3/m. Average shoreline volume change was 6, 7, and -2 m^3/m at the north, central, and southern section of the study area, respectively. R215, R215A, R217A and R220 showed loss to some degree, but all most of it was below 2 m^3/m. R216 and R218A showed more significant gains, with R218A gaining 13 m^3/m of both dry beach and shoreline. The most dynamic profile during the summer was R223 which showed loss of 15 m^3/m at the dry beach and 19 m^3/m at the shoreline.

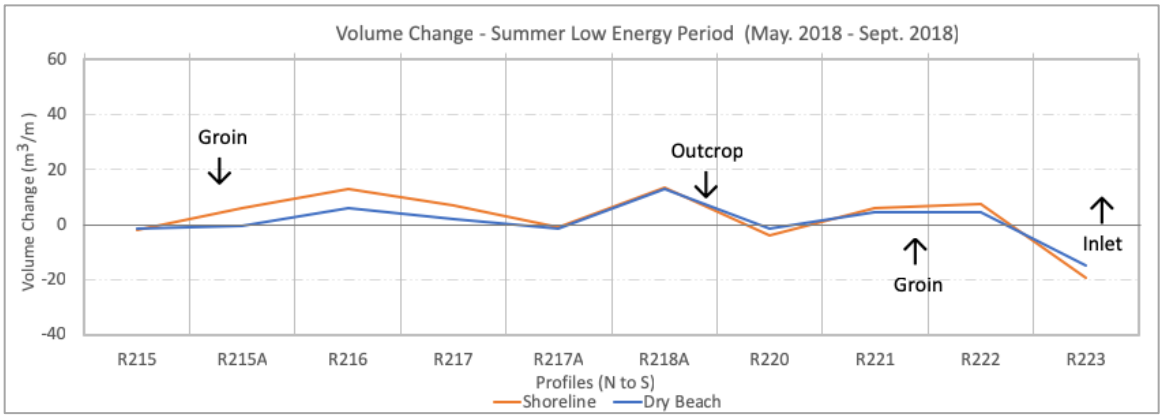

Figure 13. Volumetric change at the dry beach (+1m NAVD88) and the shoreline (0 m NAVD88) between May. 2018 and Sept. 2018. The locations of structures within the study area is indicated.

Entire Study Period (Aug. 2017 – Sept. 2018)

Average volume change at the dry beach in the north (R215 – R216) of the study area was negligible, over the center section (R217-R218A) was -12 m^3/m, and in the southern section (R220 – R223) was 8 m^3/m. Average shoreline volume change was -9, -30, and 10 m^3/m at the north, central, and southern section of the study area, respectively. Alongshore variability in volume change was significant. R215 gained 7 m^3/m in the dry beach while the shoreline volume remained stable. Erosion at R215A was 14 m^3/m in the dry beach and 30 m^3/m in the shoreline. R216 gained 8 m^3/m and 2 m^3/m in the shoreline and dry beach respectively. R217, R217A, R218A, and R220 all showed overall erosion, with R217A, the most extreme example, loosing 22 m^3/m at the dry beach and 42 m^3/m at the shoreline. In the south end of the study area R221, R222, and R223 all accreted in both the dry beach and the shoreline, with the greatest gains being at R223 (16 m^3/m at the dry beach and 33 m^3/m at the shoreline). Overall volume change during the study period reflected a general pattern of more stability with some variance in the north, erosion across the center of the study area and accretion in the south.

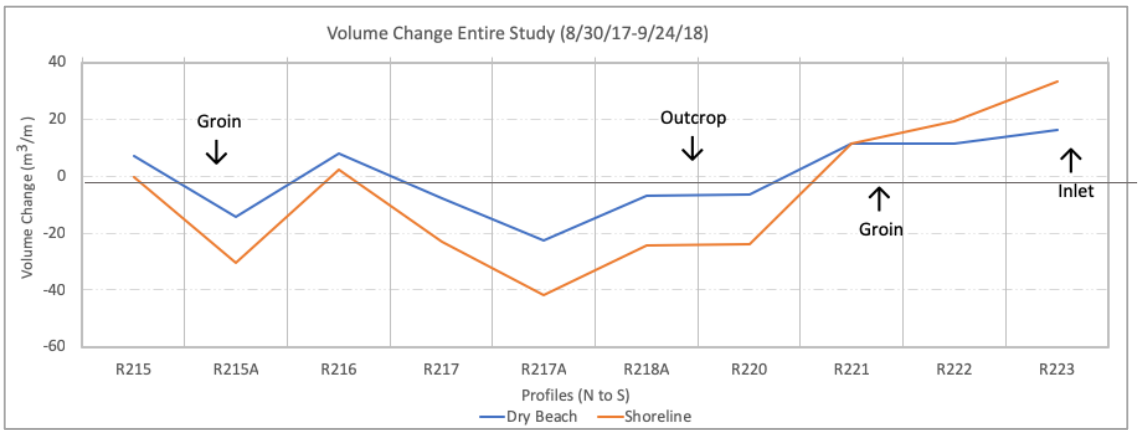

Figure 14. Volumetric change at the dry beach (+1m NAVD88) and the shoreline (0 m NAVD88) over the entire study period (Aug. 2017 – Sept. 2018). The locations of structures within the study area is indicated.

Sediment Sampling (Figure 15)

Hurricane Irma Impact (Late July 2017 – Sept. 2017)

Immediately after Irma at R215 sediment became more well sorted at the mid-beach and dune toe while grain size remained the same at each cross-shore location. At R217, R220, and R221 fining and improved sorting occurred at the mid-beach. All R223 showed no change in the dune, poorer sorting at the mid-beach, better sorting at the shoreline, with grain size stability.

Post Irma through Winter (Sept. 2017 – Feb. 2018)

By February 2018 all locations at the dune had stabilized to well sorted to moderately well sorted medium sand. A coarsening trend occurred at the mid-beach at R217, R220, and R222, removing the fine sand fraction from the study area completely, showing an alongshore trend of moderately well sorted medium sand that extended north to R215 as well. Coarsening occurred at the shoreline of R215 and the mid-beach of R223.

Winter through Summer (Feb. 2018 – Sept. 2018)

By the end of the study period coarse sand was present at the shoreline of R215, R217, and R220, showing a coarsening trend not only seasonally, but for the year. R220 showed poorer sorting at the dune and improved sorting at the mid-beach during this period, while R221's sediment remained stable. At R223 sorting got poorer at the dune toe, the mid-beach experienced coarsening, and sorting improved at the shoreline.

	R215		R217		R220		R221		R223	
7.28.17	GRAIN SIZE	DESC.	GRAIN SIZE	DESC	GRAIN SIZE	DESC.	GRAIN SIZE	DESC.	GRAIN SIZE	DESC.
DT	1.66±0.52 (ϕ)	MWS, MS	2.11±0.44 (ϕ)	WS, FS	1.65±0.67 (ϕ)	MWS, MS	1.44±0.52 (ϕ)	MWS, MS	1.43±0.58 (ϕ)	MWS, MS
MB	1.55±0.52 (ϕ)	MWS, MS	1.64±0.79 (ϕ)	MS, MS	0.97±1.74 (ϕ)	PS, CS	1.57±0.62 (ϕ)	MWS, MS	1.36±0.57 (ϕ)	MWS, MS
SL	1.39±0.57 (ϕ)	MWS, MS	1.33±0.55 (ϕ)	MWS, MS	0.87±0.92 (ϕ)	MS, CS	0.60±0.80 (ϕ)	MS, CS	1.56±0.72 (ϕ)	MS, MS
9.14.17										
DT	1.72±0.42 (ϕ)	WS, MS	1.88±0.60 (ϕ)	MWS, MS	1.84±0.55 (ϕ)	MWS, MS	1.78±0.50 (ϕ)	WS, MS	1.33±0.64 (ϕ)	MWS, MS
MB	1.17±0.42 (ϕ)	WS, MS	2.10±0.41 (ϕ)	WS, FS	2.03±0.58 (ϕ)	MWS, FS	2.02±0.44 (ϕ)	WS, FS	1.12±0.75 (ϕ)	MS, MS
SL	1.14±0.63 (ϕ)	MWS, MS	1.41±1.03 (ϕ)	PS, MS	0.62±0.82 (ϕ)	MS, CS	1.40±0.93 (ϕ)	MS, MS	1.57±0.71 (ϕ)	MWS, MS
2.26.18										
DT	1.53±.44 (ϕ)	WS, MS	1.87±0.46 (ϕ)	WS, MS	1.79±0.69 (ϕ)	MWS, MS	1.61±0.41 (ϕ)	WS, MS	1.95±0.47 (ϕ)	WS, MS
MB	1.32±0.59 (ϕ)	MWS, MS	1.68±0.66 (ϕ)	MWS, MS	1.48±0.57 (ϕ)	MWS, MS	1.62±0.51 (ϕ)	MWS, MS	0.68±0.78 (ϕ)	MS, CS
SL	0.66±0.98 (ϕ)	MS, CS	1.10±0.70 (ϕ)	MWS, MS	0.73±0.76 (ϕ)	MS, CS	1.04±0.65 (ϕ)	MWS, MS	1.16±0.59 (ϕ)	MWS, MS
7.9.18										
DT	1.33±0.64 (ϕ)	MWS, MS	1.88±0.41 (ϕ)	WS, MS	1.57±0.76 (ϕ)	MS, MS	1.91±0.42 (ϕ)	WS, MS	1.57±0.69 (ϕ)	MWS, MS
MB	1.30±0.54 (ϕ)	MWS, MS	1.42±0.53 (ϕ)	MWS, MS	1.58±0.47 (ϕ)	WS, MS	1.32±0.61 (ϕ)	MWS, MS	1.17±0.79 (ϕ)	MS, MS
SL	0.54±0.51 (ϕ)	MWS, CS	0.45±0.89 (ϕ)	MS, CS	0.64±0.62 (ϕ)	MWS, CS	1.43±0.55 (ϕ)	MWS, MS	1.61±0.48 (ϕ)	WS, MS

Figure 15. Sediment statistics from selected dates and profile locations. Dates are immediate pre and post-Irma (to reflect impact), Feb. 2018 (to reflect high energy conditions), and Sept. 2018 (to encompass the entire study). Cross-shore locations are dune toe (DT), mid-beach (MB), and shoreline (SL). Grain size and sorting are in phi, while the description column shows sorting followed by size. Sorting descriptors are well sorted (WS), moderately well sorted (MWS), moderately sorted (MS), and poorly sorted (PS). Size descriptors are fine sand (FS), medium sand (MS), and coarse sand (CS).

DISCUSSION

A summary of the Impact scale (Sallenger, 2000) and the recovery morphology in the immediate and short-term (one-year) shows considerable alongshore variability (Table 2). Several potential influences are evaluated and discussed, including the pre-storm morphology, the level of impact, and the proximity to structures organized by the spatiotemporal variability in wave climate (inferred from the local wind conditions).

Location	Irma Impact	Immediate Recovery	Dry Beach Recovery
R215	Collision	- No significant change	No loss due to Irma
R215A	Collision	- Shoreline retreat	Never recovers
R216	Overwash	- Beachface advance - Shoreline advance	Recovers by February
R217	Overwash	- Beachface - Shoreline advance	Recovers by October (recovered vol. lost by Feb.)
R217A	Collision	- Beachface advance - Shoreline retreat.	Nevers Recovers
R218	Swash	- Beachface stable - Shoreline stable	Recovers 75% within year
R220	Collision	- Beachface retreat - Shoreline retreat	Never recovers
R221	Swash	- Beachface stable - Shoreline stable	Recovers by May
R222	Collision	- Beachface retreat - Shoreline retreat	Recovers by May
R223	Swash	- Inflation above 1m elev. - Significant beachface advance	Recovers by October

Table 2. Impact, immediate recovery, and dry beach recovery characteristics

Morphology and Impact Regime

Pre-Irma beach width and slope were measured along the upper and lower portion of the profile (Figure 16). A nourishment was completed just prior to the storm in April 2017 at R217A to R223. The beach width decreased towards the lateral sections of the nourishment, but did not correspond to the determined impact regime. In addition, the lower beach slope was variable (reflective to intermediate), and also did not correspond to a particular impact regime. The southern-most location adjacent to the jetty was by far the steepest, and experienced only a swash regime. However, several other locations also were classified as swash regime but did not have the same steepness. A visual comparison of pre-storm morphology at locations classified as collision regime show little correlation between the two (Figure 17). With the exception of R222, which is a higher elevation that the others, a comparison of the pre-storm morphology of different impact regimes reveals very similar characteristics (Figure 18).

Line	description	upper slope	upper width	lower slope	lower width	impact regime	structure
R215	upper flat, sloped lower	1/75	15 m	1/8	16	collision	N. of groin
R215A	sloping upper and lower	1/25	25 m	1/9	12 m	collision	S. of groin
R216	sloping upper and lower	1/25	35 m	1/7	14 m	overwash	
R217	upper is stepped	1/29	40 m	1/12	18.4 m	overwash	
R217A	upper is flat, lower has berm	1/76	42 m	1/10	26 m	collision	
R218A	upper is flat with rise, lower has berm	1/120	40 m	1/9	21 m	swash	
R220	upper is flat, lower has berm	1/86	50 m	1/9	27m	collision	S. of outcrop
R221	upper sloped, lower has berm	1/27	36 m	1/12	25 m	swash	N. of groin
R222	steady curve across beach	1/27	31 m	1/11	20 m	collision	S. of groin
R223	upper sloped, lower steep with berm	1/15	12 m	1/3	6 m	swash	N. of jetty

Figure 16. Pre-Irma beach morphology, impact regime, and structural influence.

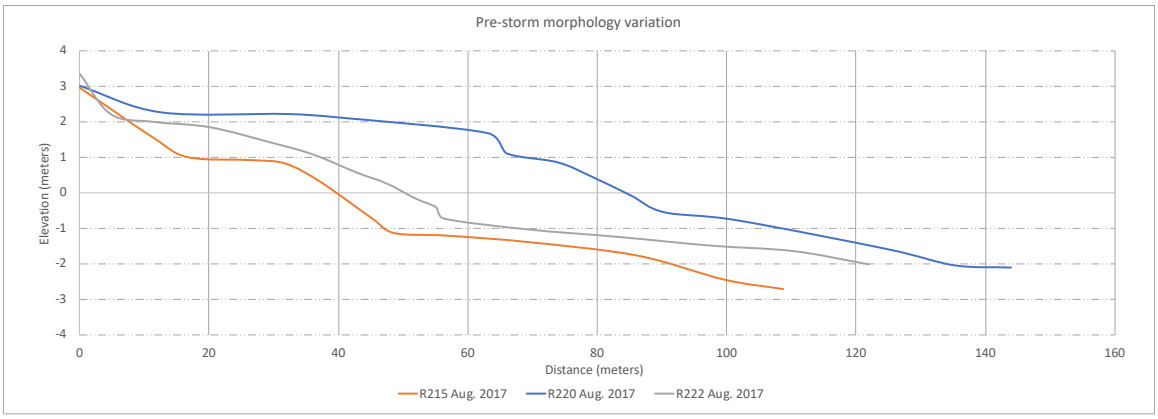

Figure 17. Pre-storm morphology at R215, R220, and R222. Very different morphologies are exhibited while all experienced a collision regime.

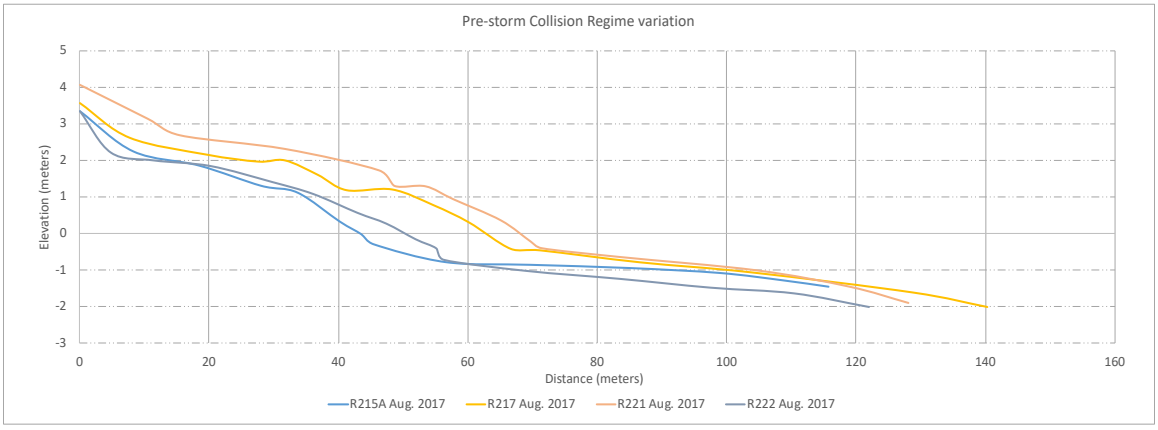

Figure 18. Pre-storm morphology at R215A (collision), R217 (overwash), R221 (swash), and R222 (collision). Each shows a similar pre-storm morphology while exhibiting different impact regimes.

Despite the variability in the beach width, slope, and impact scale, a typified storm impact and recovery morphology of a deflated beach with nearshore deposition and in many cases some backbeach deposition accounts for nearly 90 % of the general post-storm morphology (Figure 19). The exception to this rule was R223, which is just north of the jetty. Here the sediment seems to have been moved down the profile where the beachface, shoreline, and nearshore showed advance. Proximity to the jetty influences

nearly all surveys dates on this transect and the jetty seems to impound sediment for much of the year.

The more extreme volume loss measured at R215A vs. R215 (a 20 m^3/m difference), which are only separated by 400 m, is also an example of the influence a structure may have on a section of beach. The highest volume losses in the study area were in the center at R217A and R218A (at ~27 m^3/m), establishing a pattern of primarily erosive behavior in that section of beach. The fining of sediment samples on the mid-beach at R217, R220, and R221 is indicative of high-water levels impacting the sediment characteristics at those locations, changing the normal composition of moderately well sorted medium sand to more well sorted finer sediment.

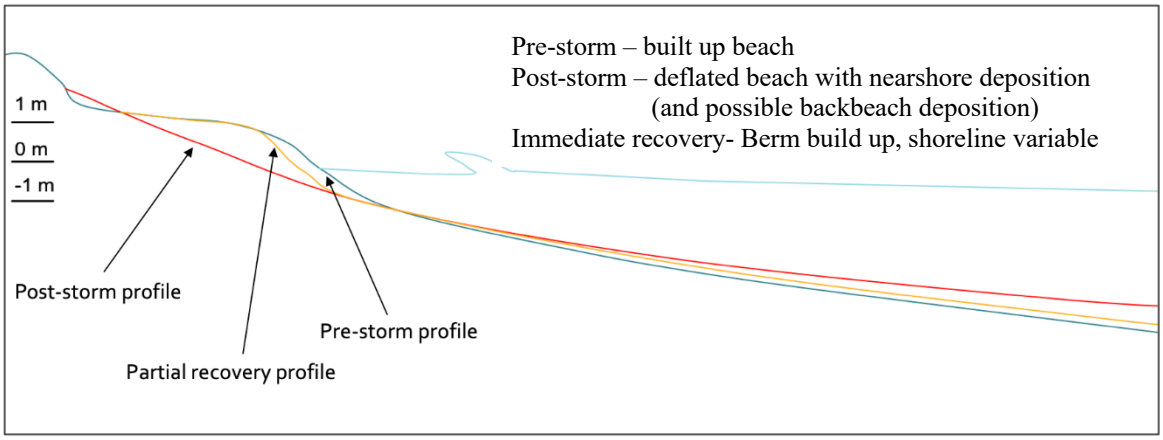

Figure 19. Conceptual diagram of typified profile impact response and immediate recovery.

Immediate Recovery Morphology

Although the morphology of impact and recovery was similar, the timing of the beach evolution varied. During the immediate post-storm recovery period, only 50 % of the profiles in the study area reflected the conceptualized recovery regime, with berm build up from cross-shore redistribution of nearshore storm deposits. The remaining 50 % of the profiles responded differently due to their location in relation to structure or

alongshore location in relation to areas of varying hydrodynamics. Shorelines remained predominantly variable. A second-high water event caused by perigean spring tides (PST) occurred between Sept. 18th and 20th, with surge approaching 0.3 m above predicted values. This second high-water event, although not accompanied by high winds, likely had an effect on the early recovery. Although elevated water alone does not affect morphodynamics, it does extend the elevation with which the waves and currents operate on, moving the accretive or erosive forces to higher than usual elevations.

Overall most profiles showed inflation, accretion, and advance, recovering sediment along the entire profile. Loss of volume and erosion across the entire profile was measured at R215A and R220. Both of these profiles have a structure to the north, suggesting the inhibition of longshore sediment transport (LST) that was acting as one of the drivers for recovery throughout the system. R215, R217A, and R222, although gaining volume, showed retreat at the shoreline. The greatest gains (in volume and profile accretion) were seen at R223 (jetty adjacent), supporting the idea that southward LST was a driver of the recovery. The second greatest volume gain was at R217, which is located in the north of the central section of the study area, an area that had established itself with the greatest volume loss immediately post-Irma.

Early Winter Morphology Evolution

Between Oct. and Dec. 2017, meteorologic conditions varied more, with high water conditions occurring during storms and the PST events of October and November. October's water level reached nearly the same elevation as Hurricane Irma's, with correspondingly high onshore winds (Figure 20). Morphology during this period showed profile retreat and volume loss in the north and center of the study and gain in the south.

Fairly significant loss was measured at the middle profiles (R216, R217, and R217A) which are unaffected by structures and experienced recovery during the 1st month after the storm. Conversely, R220 and R221, which had eroded and remained unchanged during the 1st month of recovery reversed, accreting and advancing. Coupling the meteorologic and with morphologic data suggest the temporally extended high energy conditions continued to cause heavy erosion on the middle area of the study while LST moved that sediment south, making it available to these profiles. As the pattern for these profiles has been reversed between these time periods it is likely that offshore volume lost during the hurricane was gained back immediately post-storm in the north, making it available to be eroded with the high energy conditions of the winter. The opposite would be true in the south; the sediment was not recovered immediately post-storm, and subsequently the high energy conditions of early winter mobilized it and helped the beach recover.

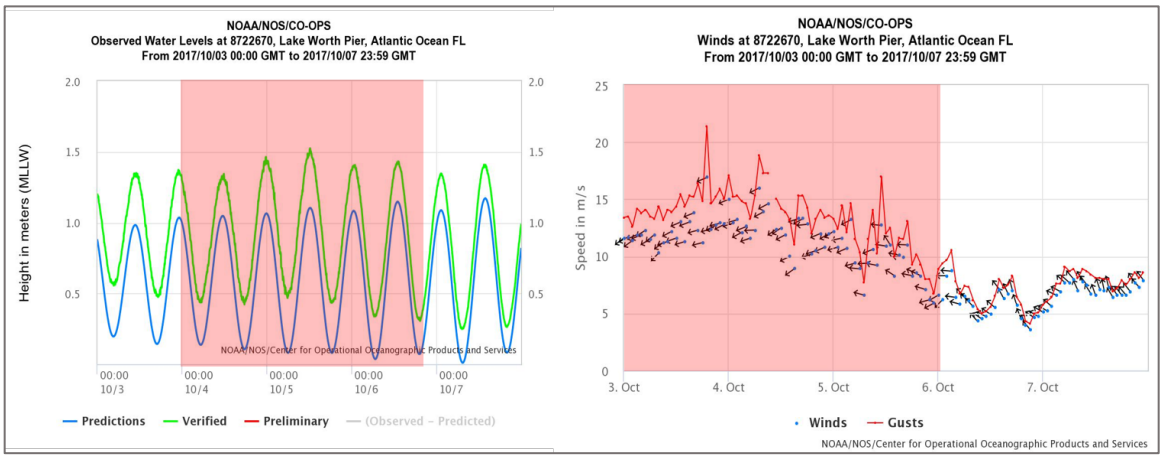

Figure 20. NOAA Tides and Currents data for Oct. 3 – Oct. 7, showing a period of high energy not associated with a PST event. Water levels reach nearly that of Hurricane Irma (NOAA, 2019).

Mid-Winter Morphology Evolution

Overall morphology between December 2018 and February 2018 showed not only alongshore variability within the study area but greater cross-shore variability within profiles between surveys. High energy conditions were present in early January, with a weather event impacting the shore with surge levels 0.4 m above predicted values and NE sustained winds exceeding 30 mph for 24 hours (Figure 21). At R215 and R215A backbeach gains that had appeared in Dec., likely from high water deposition were eroded and redistributed to the dry beach, beachface, and shoreline. R216 showed significant advance, continuing its recovery from Irma. R217, R217A, R218A and R220 all showed retreat and volume loss, with a steep nearly 1 m scarp forming at R217 and R218A (Figure 7), a signifier of erosive conditions. Between October and February R217 lost 17 m^3/m of volume above 1 m elevation, establishing it as a profile outlier in volume change. The overall behavior of the central section of the study area (R217, R217A, and R218A) during this time period of erosion and volume loss, decreasing moving southward, again points to it as an erosional hotspot in which R218A is the southern extent. R220's morphology is particularly interesting here. Immediately post-Irma it was one of the only locations that continued to retreat over the entire profile, while in Dec. it had measured significant advance (Figure 22). Then, in February it showed retreat at the shoreline and beachface, but accretion in the backbeach. Its behavior does not match that of either nearby profiles or any other profiles that are located south of a structure. Cross-shore morphodynamics are clear at this location; in times of shoreline retreat the backbeach is inflated and vice-versa. Sediment samples from the location are not abnormal in any way. Advance and accretion were measured on

both sides of the groin at R221 and R222. At R223 significant cross-shore variability from the previous survey was measured. The upper beach inflated by 1 m with dry beach volume gains of over $20 m^3/m$ with the shoreline and beachface retreating by 4 m. At this location, it seems that the erosive effect of the winter high energy conditions moved the sediment to the upper part of the profile as the jetty prevents it from leaving the system. Sediment samples from this time show a coarsening at the mid-beach of R217, R220, and R221, indicative of redistribution of the post-Irma fine sediment.

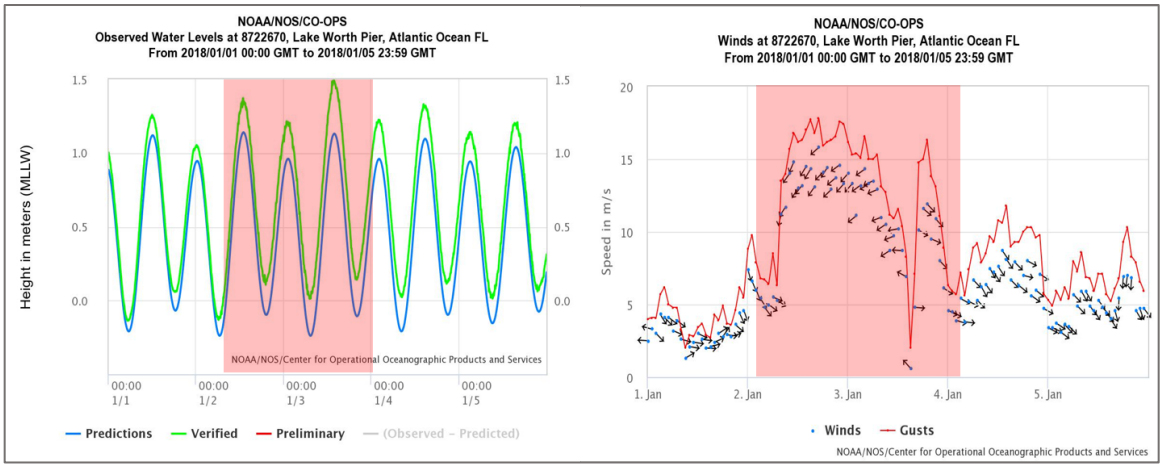

Figure 21. NOAA Tides and Currents data for Jan. 1 – Jan. 5, showing a period of high energy not associated with a PST event. Water levels reach nearly that of Hurricane Irma (NOAA, 2019).

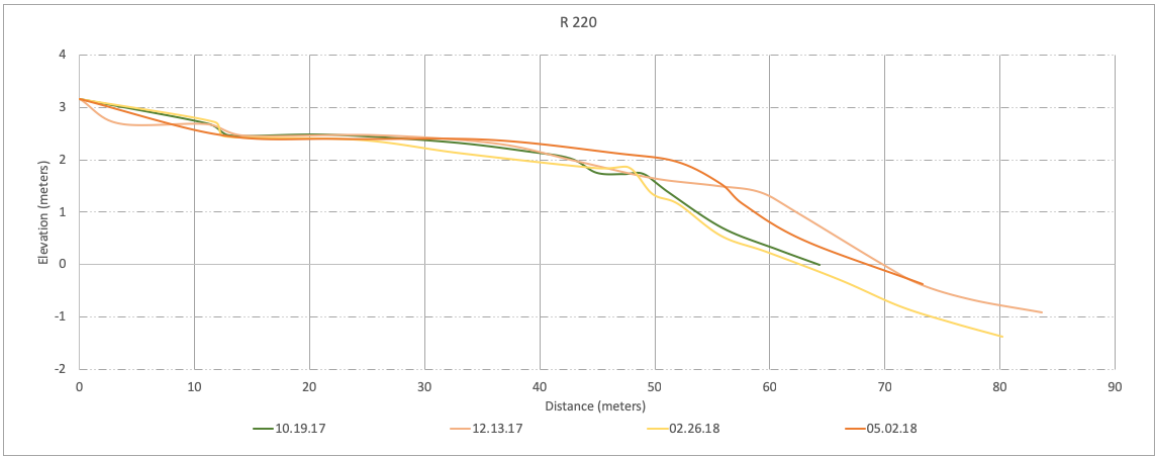

Figure 22. Cross-shore variability in R220 between Oct. 2017 and May 2018. The profile exhibits an alternating patter of gain and loss that is not exhibited by other profiles during that time. R220 is south of the outcrop.

Late Winter Morphology Evolution

Between February and May 2018, there were no significant meteorologic forcing conditions and the study area averaged 4 m^3/m dry beach volume gain. In the north (R215 – R216) the average dry beach gain was 4 m^3/m, in the central section (R217 – R218A) the average dry beach gain was 3 m^3/m, and at the southern section (R220 – R223) the average dry beach gain was 5 m^3/m. This overall slight gain in dry beach volume confirms the meteorological data that shows it was a calm late winter. Much of the variability in this time period was cross-shore movement of beachface and shoreline sediment to the upper beach. In center of the study area the scarp that appeared at R217 and R218A was flattened through different mechanisms. R217's scarp deflated (erosion), while at R218A the scarp was buried (accretion) (Figure 23). This varied response of a similar feature under the same conditions (no structure and same meteorologic conditions) confirms that R218A is on the southern end of the erosional hotspot. R220's morphology, previously not following other morphological patterns of the study area, advances and inflates, becoming similar to nearby profiles. Deflation at R223 above 2 m

elevation with slight shoreline advance shows that with a calmer winter sediment eroded and made available for LST is less, therefore less is available to be impounded at R223. R215A, with shoreline retreat, and R223, with upper beach deflation, exhibited different morphologies from the rest of the study area due to being structure adjacent and the effect that the structure has on LST. Interestingly R220 and R222, two other profiles directly affected by structures, responded to this period like the majority of the study area. Both are south of their respective structures. The outcrop north of R220 may not extend far enough offshore to always restrict sediment flow, while the permeability of the groin north of R222 likely contributes to the less extreme responses seen there as compared to R215.

As a period of primarily upper beach inflation, shoreline stability or advance (in most cases), and average volume gain, late winter appears to be a period of recovery. Meteorologic conditions, being abnormally calm for the season, allowed this to happen.

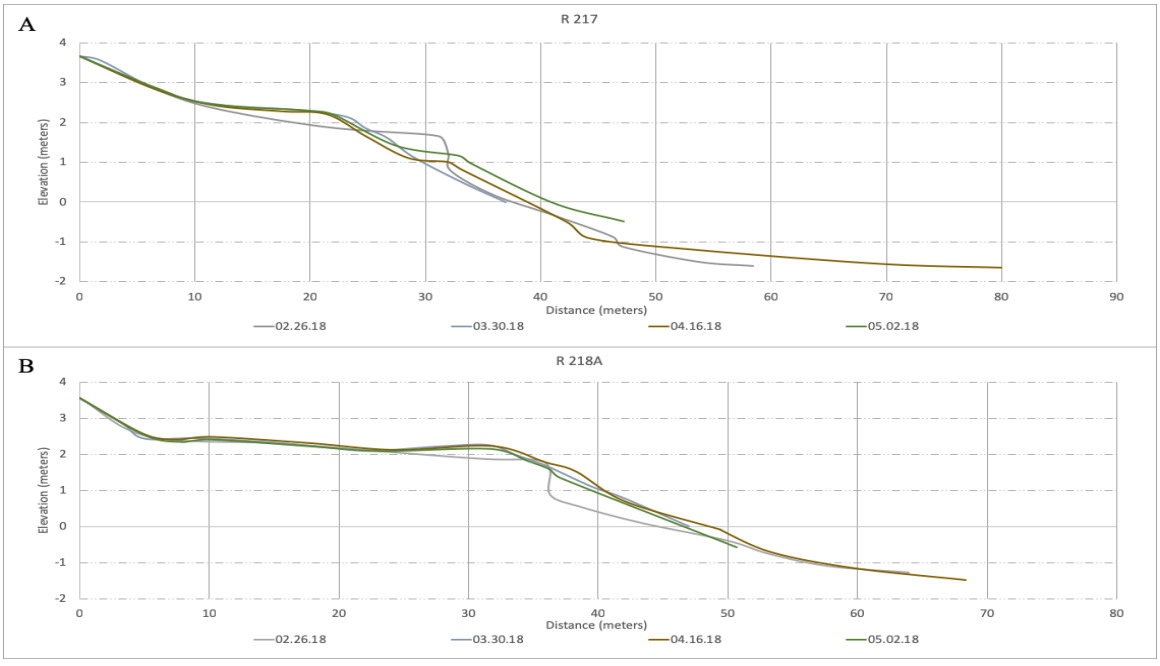

Figure 23. (A)R217 and (B)R218A between Feb. and May, showing the February scarp flattening with different mechanisms, erosion at R217 and accretion at R218A.

Summer Morphology Evolution

The summer of 2018, May to September, was typified by relative volume stability throughout the study area. Summer conditions allowed for longer surveys to be completed, mapping nearshore deposition in much of the study area as the summer progressed. Average dry beach volume change in the north (R215 – R216) was -0.5 m^3/m, in the center (R217 – R218A) was 2 m^3/m, and in the south was -2 m^3/m. Profile behavior was generally that of beachface and shoreline stability or gain, with variability in the early and late summer attributed high wind events in late May and Sept. and a PST event in mid Sept. Sustained winds, between May 27 and May 29, exceeded 25 mph directly out of the south for nearly 48 hours. These conditions attributed to erosional berm and scarp formations at R215, R215A, R216, R218A, R220, and R222. R215A, R220, and R222 are on the south side of structures. Scarp formation at these locations can be attributed to the exposure to the directionality of the waves created by the strong south wind. R221, just north of the groin that R222 is affected by, did not show the same erosive behavior during this storm as it was protected from the predominant wind and wave direction. Erosion was measured along most of the study area after this event, with most profiles returning to their early-May shape by September.

Overall during the lower energy summer R215A exhibited cross-shore variability, with a berm moving seaward through the summer, further showing that the influence of proximal structures is the primary driver of morphology at this location. R216 show, R217, and R217A show relative stability to growth during the summer. R217 and R217A, which had been an erosional hotspot for the majority of the study stabilize, suggesting that winter conditions and LST direction may contribute that section of the

beach's erosion. More variability occurred in the south of the study area, with R218A, R220, and R223 loosing beachface and shoreline throughout the summer.

A PST event occurred between Sept. 7 – 10 (Figure 24) and a separate high wind event occurred earlier in the month (with winds from the ESE). Both occurred before the September survey date, allowing their impact to be measured. Retreat at R218A, R220, and R223 measured in September can be attributed to these elevated conditions as previous surveys completed in June and July show advance at these profiles. R221 and R222, on either side of the groin responded similarly to the September conditions. This is in contrast to the May high wind event where they differed in response. May's winds were almost directly out of the south, while in September the wind direction was more or less onshore, suggesting that it takes highly shoreline lateral winds to bring this groin into play as a driver of adjacent morphology. R223's morphology during the summer was that of retreat directly after the May high wind event, with deflation in the upper beach as well. The reversal of LST during the summer is evident here and it is likely that this profile was starved for sediment, making it difficult to recover from losses that occur in the late winter and early summer.

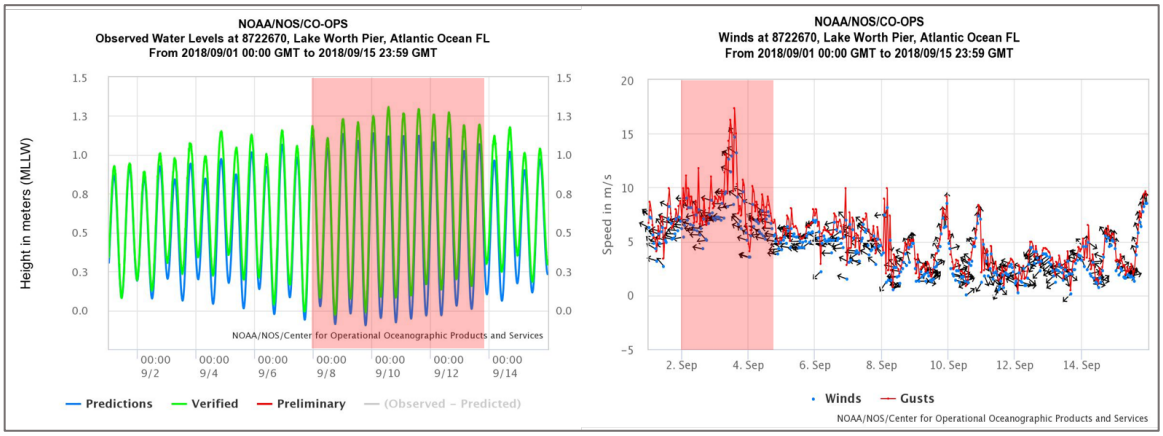

Figure 24. NOAA Tides and Currents data for the Sept. 7-10 PST event (left) and Sept. 2-5 high wind event (right) (NOAA, 2019).

Overall Recovery (Pre-Irma – Sept. 2018)

Over the study area, after a year of impacts including a hurricane and multiple high water and wind events, there was significant alongshore variability in recovery. Profile morphology for the year is that of a generalized pattern of retreat and erosion in the north and central sections and advance and accretion in the south, showing the significant influence LST has in the study area. R215's morphodynamics for the year showed back-beach aggradation and beach-face and shoreline retreat, with the profile becoming more monotonic in 2018. At R215A, which showed great cross-shore variability throughout the year, the profile appears similar and slightly steeper but severely retreated in the summer of 2018. Beginning at R216 moving south a pattern of erosion is present, with R217A, R218A, and R220 showing similar morphological behavior between Aug. 2017 and Sept. 2018. At R221 this pattern reverses itself, with advance and accretion increasing to R223, showing that this is the location where eroded sediment transported from the north of the study begins to return to the subaerial profile. Sediment samples between to two years show little consequential variation, although there is coarsening of shoreline sediment at R215 and R217.

Volume change over the study showed similar alongshore variability. In the north of the study area (R215 – R216) average volume change at the dry beach was 0.3 m^3/m and at the shoreline was -9 m^3/m, with the most significant losses at R215A, showing the long-term effect that the groin and hard bottom have at this location. In the center (R217 – R218A) average volume change was -12 m^3/m at the dry beach and -30 m^3/m at the shoreline. These profiles especially R217 and R217A, experience volume losses and

shoreline retreat unlike any other locations in the study. Scarp formation tends to be more common in this area as well (evident between R217 and R218A in Feb. 2018). This area of the beach is uninfluenced by structures, therefore is an erosional hotspot, predominantly showing morphologic behavior that diverts from the norm during much of the study. Also, when considering volume changes at R217 moving south, the effect the recent nourishment would have had must be recognized. A greater quantity of sediment on the post-nourishment, pre-storm equilibrated profiles, would have been available to be eroded, increasing the volume loss seen in the central section, and contributing to the sediment available to the southern section of the study area. In the south of the study area, between R220 and R223 the average volume change was 8 m^3/m at the dry beach and 10 m^3/m at the shoreline Volume increases in the south at R221, R222, and R223, suggests that the jetty and groin present impound sediment transported alongshore seasonally and provide protection from long-term erosion.

When looking specifically at the volume change post-Irma and the rate at which the beach recovered, in the north and center of the study area variability was measured, while the south recovered volume quickly (Figure 25). Above the 1 m elevation contour R215 gained immediately back what was lost and accreted throughout the year. R215A never gained back what was lost during Irma, with little volume change after the impact. R216 had gained back most of what was lost by Feb. 2018 and accreted throughout the study. R217 gained over 200% percent of the dry beach volume lost by Oct. 2017 and by Feb. 2018 had lost it all back again, never recovering. R217A, showing the greatest dry beach volume loss during the storm recovered some volume through the study, but very little. R218A increasingly recovered throughout the study, and by September 2018 had

recovered 75% of volume lost due to Irma. R220 had not fully recovered by the end of the study, recovering only 46% of what was lost. R221, R222, and R223 all showed volume gain by Oct., nearly full recovery by Feb., and by Sept. 2018 recovered 170%, 220%, and 320% of the volume lost due to Irma (respectively), clearly quantifying the disproportionate recovery pattern from north to south.

Patterns repeated in these recovery rates reiterate the effect of structure and LST on volume change. R215 and R215A (on the north and south of the same groin) show gain in the north and loss in the south. R220, south of the outcrop, never fully recovers, and R223, north of the jetty, shows volume gains far exceeding that of the other locations. The effect that adjacent structure had on these locations directly shows the influence that LST had on the recovery. Profiles north adjacent to structure had overall volume increase while the locations on the south had overall erosion. Predominant LST direction during the study was north to south, and when it did reverse during the summer, supporting evidence emerged of both the role that LST and structures played. Summer volume losses, although to different degrees, were measured at both R215 and R223, both north of the structures that previously contributed to their accretion and advance. The lack of notable recovery at R217 and R217A, coupled with the greater post-storm volume losses at R217A and R218 point to evidence of this as an erosional hotspot and the possibility that greater volume changes were subject to greater post-nourishment sediment availability. When considering alongshore and cross-shore variability, especially within this erosional hotspot, the presence of offshore patch reefs and the exposed antecedent geology of the Anastasia Formation clearly play a role in the hydrodynamic forces that influence the beach.

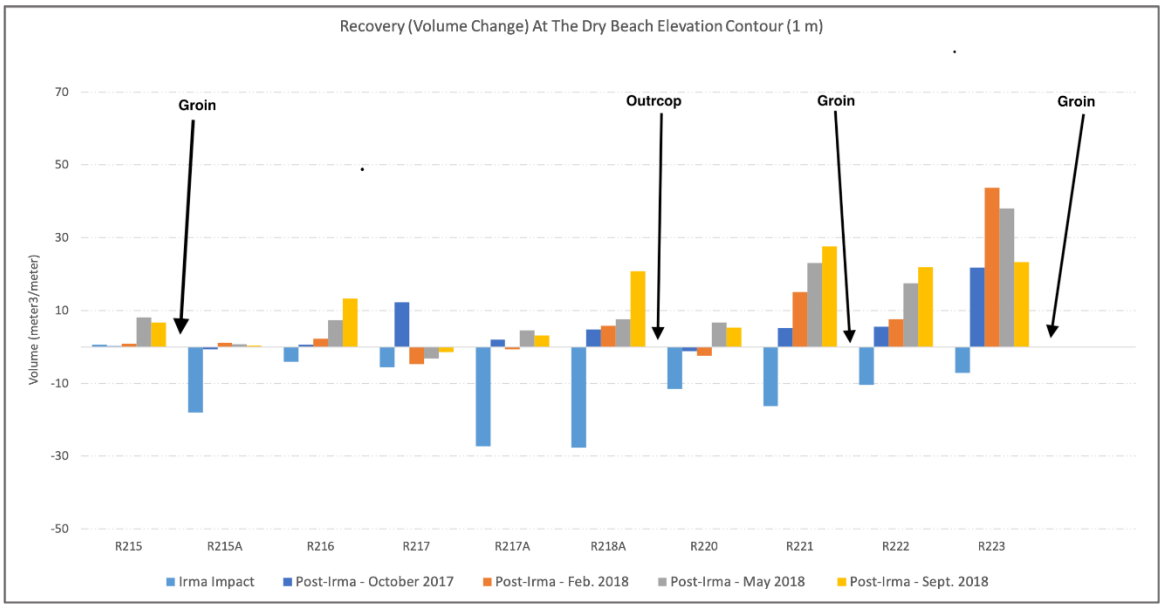

Figure 25. Recovery volume change at the 1 m elevation contour following Hurricane Irma, delineated by seasons.

CONCLUSIONS

This study uses time-series beach profiles, meteorologic conditions (including water level and wind speed), and cross-shore sediment samples collected at the surface to evaluate short-term (one year) morphologic evolution of post-storm recovery following Hurricane Irma. The objectives of this study were to 1) classify the storm impact regime due to Hurricane Irma, and 2) quantify short-term (i.e., up to 12 months post-storm) recovery morphology and rate of recovery. Understanding beach response and recovery to storms is critical for effective mitigation efforts and conserving the coastal zone for future use.

Perigean spring tides and energetic wind conditions accounted for extended temporal variability that affected the ability of the beach to recover its pre-Irma shape and volume. The occurrence of alongshore variability is attributed to the expected effects of longshore sediment transport and the presence of the 2 groins, an outcrop, and jetty present in the study area, as well as the appearance of an erosional hotspot in the central section. The study area's recovery was primarily dependent upon rates of longshore sediment transport, highly localized hydrodynamic conditions, weather patterns following the storm (Figure 3, 4, 5), and the structures adjacent to certain profiles (Figure 2). Immediate recovery (by October) and whether or not a location recovered completely are dictated primarily by these variables, with impact regime and pre-storm morphology playing little role (Table. 2).

The storm impact regimes resulting from Hurricane Irma ranged from swash to overwash. In general, planar nearshore deposition, as opposed to sandbar formation, was exhibited, marking a behavior more commonly seen in mixed sand and gravel beaches. The overwash regime did not represent increased erosive forces or result in a more extreme impact, but rather deposition in the dunes and backbeach. Pre-storm morphology played little to no role in impact regime at a location. Individual profile response to the storm impact and it's recovery was dictated not only by the level of the impact itself, but by the wind and water levels that drove the recovery process, longshore sediment transport patterns, the profile's location within the study area, and proximity to structures. 50 % of the profiles exhibited typified immediate recovery, aided by perigean spring tides that occurred within 10 days following Hurricane Irma. Those that did not were influenced by structure, LST, and localized hydrodynamics.

Structural influence is closely tied to longshore sediment transport, which had the greatest impact the rate at which profiles recovered. Significant volume gains in the south, coupled with known LST direction and summer reversal of trends confirm this. Secondly, it can be seen that temporally extended high energy conditions impact recovery rate and scope. High water levels alone tended to help deposit sand in the upper beach, while high wind conditions, which drive breaking waves, coupled with high water, had and erosive effect seen during periods when scarp formation was measured. The presence of an erosional hotspot in the middle of the study area is a result of highly localized hydrodynamic conditions, as no structures are present in the area. Offshore patch reefs and the proximity of the Anastasia Formation (exposed as hardbottom at R215A and the outcrop north of R220) likely contribute to this areas morphodynamic,

and as soon as the sediment is removed by these localized conditions LST plays its role, moving the sediment away from the area. The Sallenger Storm Impact scale, a common metric is assessing storms impacting barrier islands may not be appropriate at this local spatial scale, where other factors, such as alongshore variability in hydrodynamics due to geology, may be more of an influence.

Future research is needed to extend the study temporally forward, to follow the evolution through another year. Also, Boca Raton is regularly nourished, and previous studies found that Hurricane Irma equilibrated nourished profiles (Shahan, 2018). Encompassing the morphologic behavior of this beach, including the nourishment, impact (equilibration) period, and recovery period would create a comprehensive picture of Boca Raton's beach in response to all of its primary morphologic drivers, including mitigation measures. Localized studies of the central section of the study area would integral in understanding the erosional hotspot measured there. Wave modeling in conjunction with detailed reef maps would be an essential tool for this. A study based on R223 and how it responds to the inlet's dynamics during ebb and tidal stages would help to explain its role within the littoral cell. Also, extending a study north, to look specifically at sediment transport quantity and rate would help develop a greater understanding of how the entire area responds to impact and the way in which it recovers. Overcoming limitations in current monitoring methods would help identify nearshore sediment patterns more clearly, as identifying bathymetric variation would increase cross-shore profile accuracy and aid in volumetric analysis.

By establishing a fundamental understanding of the evolution of this beach during a storm recovery period, with consideration to location specific driving forces, proactive

measures and response plans can be tailored more effectively. The use of more effective measures, pre and post-storm, will not only save money and time (by way of less intensive beach nourishment and protection projects), but will help to provide a more sustainable buffer to future variability.

REFERENCES

Ba, A., & Senechal, N. (2013). Extreme winter storm versus Summer storm: morphological impact on a sandy beach. *Journal of Coastal Research*, *65*(65), 648–653. https://doi.org/10.2112/SI65.110.1

Benedet, L., Finkl, C. W., & Hartog, W. M. (2007). Processes Controlling Development of Erosional Hot Spots on a Beach Nourishment Project. *Journal of Coastal Research*, *231*(1), 33–48. https://doi.org/10.2112/06-0706.1

Benedet, L., Finkl, C. W., & Klein, a H. F. (2006). Morphodynamic classification of beaches on the Atlantic coast of Florida: Geographical variability of beach types, beach safety and coastal hazards. *Journal of Coastal Research*, *1*(39), 360–365

Biausque, M., Senechal, N., Blossier, B., & Bryan, K. R. (2016). Seasonal Variations in Recovery Timescales of Shorelines on an Embayed Beach. *Journal of Coastal Research*, *75*(sp1), 353–357. https://doi.org/10.2112/SI75-071.1

Brenner, O. T., Lentz, E. E., Hapke, C. J., Henderson, R. E., Wilson, K. E., & Nelson, T. R. (2018). Characterizing storm response and recovery using the beach change envelope: Fire Island, New York. *Geomorphology*, *300*, 189–202. https://doi.org/10.1016/j.geomorph.2017.08.004

Browder, A. E., & Dean, R. G. (2000). Monitoring and comparison to predictive models of the Perdido Key beach nourishment project, Florida, USA. *Coastal Engineering*, *39*(2–4), 173–191. https://doi.org/10.1016/S0378-3839(99)00057-*5*

Coco, G., Senechal, N., Rejas, A., Bryan, K. R., Capo, S., Parisot, J. P., … MacMahan, J. H. M. (2014). Beach response to a sequence of extreme storms. *Geomorphology*, *204*, 493–501. https://doi.org/10.1016/j.geomorph.2013.08.028

Dean, R. (2002). *Beach Nourishment Theory and Practice*. Hackensack, NJ: World Scientific Publishing Co.

Dolan, R., & Davis, R. E. (1992). An Intensity Scale for Atlantic Coast Northeast Storms. *Journal of Coastal Research*, *8*(4), 840–853Durán, R., Guillén, J., Jiménez, J. A., Sagristà, E., & Ruiz, A. (2016). Morphological changes, beach inundation and overwash caused by an extreme storm on a low-lying embayed beach bounded by a dune system (NW Mediterranean). *Geomorphology*, *274*, 129–142. https://doi.org/10.1016/j.geomorph.2016.09.012

Elko, N. A. (2005). Management of a beach nourishment project during the 2004 hurricane season. *Shore & Beach*, *73*(2), 49–54.

Elko, N. A., & Wang, P. (2007). Immediate profile and planform evolution of a beach nourishment project with hurricane influences. *Coastal Engineering*, *54*(1), 49–66. https://doi.org/10.1016/j.coastaleng.2006.08.001

Florida Department of Environmental Protection. (2015). Critically Eroded Beaches in Florida. *Florida Department of Environmental Protection*, (June), 1–76.

Florida, USA. *Coastal Engineering*, *70*, 21–39. https://doi.org/10.1016/j.coastaleng.2012.06.003

Hamm, L., Capobianco, M., Dette, H. H., Lechuga, A., Spanhoff, R., & Stive, M. J. F. (2002). A summary of European experience with shore nourishment. *Coastal Engineering*, *47*(2), 237–264. https://doi.org/10.1016/S0378-3839(02)00127-8

Houser, C., & Greenwood, B. (2007). Onshore Migration of a Swash Bar During a Storm. *Journal of Coastal Research*, *231*, 1–14. https://doi.org/10.2112/03-0135.1

Houser, C., Hapke, C., & Hamilton, S. (2008). Controls on coastal dune morphology, shoreline erosion and barrier island response to extreme storms. *Geomorphology*, *100*(3–4), 223–240. https://doi.org/10.1016/j.geomorph.2007.12.007

Houser, C., Wernette, P., Rentschlar, E., Jones, H., Hammond, B., & Trimble, S. (2015). Post-storm beach and dune recovery: Implications for barrier island resilience. *Geomorphology*, *234*, 54–63. https://doi.org/10.1016/j.geomorph.2014.12.044

Inman, D.L., and Nordstrom, C.E., 1971. On the tectonic and morphologic classification of coasts. Journal of Geology 79, 1-21.

Komar, P. D. (1998). Beach Morphology and Sediment. In *Beach Processes and Sedimentation* (pp. 45–75). Upper Saddle River, New Jersey: Prentice Hall.

Kraus, N. C., Mcdougal, W. G., Kraust, N. C., & Mcdougalt, W. G. (1996). The Effects of Seawalls on the Beach: Part I, An Updated Literature Review. *Source: Journal of Coastal Research Journal of Coastal Research Journal of Coastal Research*, *12*(123), 691–701. https://doi.org/10.2307/4298517

Kraus, G. (2001). Beach Erosional Hot Spots: Types, Causes, and Solutions. *Solutions*, (September), 1–17

Lee, J.-M., Park, J.-Y., & Choi, J.-Y. (2016). Evaluation of Sub-aerial Topographic Surveying Techniques Using Total Station and RTK-GPS for Applications in Macrotidal Sand Beach Environment. *Journal of Coastal Research*, *65*(65), 535–540. https://doi.org/10.2112/si65-091.1

Maspataud, A., Ruz, M., & Hequette, A. (2009). Spatial Variability in Post-Storm Beach Recovery along a Macrotidal Barred Beach. *Journal of Coastal Research*, *1*(56), 88–92.

de Meijer, R., Bosboom, J., Cloin, B., Katopodi, I., Kitou, N., Koomans, R., & Manso, F. (2002). Gradation effects in sediment transport. *Coastal Engineering*, *47*(2), 179–210. https://doi.org/10.1016/S0378-3839(02)00125-4.

Morton, R. A., Paine, J. G., & Gibeaut, J. C. (1994). Stages and Durations of Post-Storm Beach Recovery, Southeastern Texas Coast, U.S.A. Author (s): Robert A. Morton, Jeffrey G. Paine and James C. Gibeaut Published by: Coastal Education & Research Foundation, Inc. Stable URL: http://www.jst. *Journal of Coastal Research*, *10*(4), 884–908.

NOAA. (2016A). *Wavewatch III model*. Retrieved from http://polar.ncep.noaa.gov/waves/wavewatch/

NOAA Tides & Currents. (2019). Retrieved March 13, 2019, from http://www.tidesandcurrents.noaa.gov/

Pontee, N. (2013). Defining coastal squeeze: A discussion. *Ocean and Coastal Management*, *84*, 204–207. https://doi.org/10.1016/j.ocecoaman.2013.07.010

Roberts, T. (2012). *Natural and Anthropogenic Influences on the Morphodynamics of Sandy and Mixed Sand and Gravel Beaches*. University of South Florida.

Roberts, T. M., & Wang, P. (2012). Four-year performance and associated controlling factors of several beach nourishment projects along three adjacent barrier islands, west-central

Roberts, T. M., Wang, P., & Puleo, J. A. (2013). Storm-driven cyclic beach morphodynamics of a mixed sand and gravel beach along the Mid-Atlantic Coast, USA. *Marine Geology*, *346*, 403–421. https://doi.org/10.1016/j.margeo.2013.08.001

Schambach, L., Grilli, A. R., Grilli, S. T., Hashemi, M. R., & King, J. W. (2018). Assessing the impact of extreme storms on barrier beaches along the Atlantic coastline: Application to the southern Rhode Island coast. *Coastal Engineering*, *133*(June 2017), 26–42. https://doi.org/10.1016/j.coastaleng.2017.12.004

Scott, T., Masselink, G., Poate, T., Russell, P., Davidson, M., & Conley, D. (2016). The extreme 2013/2014 winter storms: Hydrodynamic forcing and coastal response along the southwest coast of England. *Earth Surface Processes and Landforms*, *41*(3), 378–391. https://doi.org/10.1002/esp.3836

Senechal, N., Coco, G., Castelle, B., & Marieu, V. (2015). Storm impact on the seasonal shoreline dynamics of a meso- to macrotidal open sandy beach (Biscarrosse, France). *Geomorphology*, *228*, 448–461. https://doi.org/10.1016/j.geomorph.2014.09.025

Shahan, T. (2018). *Morphologic Evolution And Alongshore Variability Of Two Beach Nourishment Projects In Southeast Fl., USA*(Unpublished master's thesis). Florida Atlantic University.

Shahan, T., & Briggs, T. R. (2017). Morphologic evolution of a small nourishment project in Boca Raton, Florida, USA. *Shore and Beach*, *85*(3), 1–10. Retrieved from methods, morphology, survey,

Short, A. D. (1999). Beaches. In A. D. Short (Ed.), *Handbook of Beach and Shoreface Morphodynamics* (pp. 3–20). West Sussex, England: John Wiley & Sons, Ltd.

Splinter, K. D., Strauss, D. R., & Tomlinson, R. B. (2011). Assessment of post-storm recovery of beaches using video imaging techniques: A case study at Gold Coast, Australia. *IEEE Transactions on Geoscience and Remote Sensing*, *49*(12 PART 1), 4704–4716. https://doi.org/10.1109/TGRS.2011.2136351

Stauble, D. K., & Kraus, N. C. (1993). Beach nourishment engineering and management considerations. ASCE.

US Department of Commerce, National Oceanic and Atmospheric Administration. (2014, August 01). What is a perigean spring tide? Retrieved November 21, 2017, from https://oceanservice.noaa.gov/facts/perigean-pring-tide.html

Wentworth, C. K. (1922). A Scale of Grade and Class Terms for Clastic Sediments. *The Journal Of Geology,30*(5), 377-392

Yu, F., Switzer, A. D., Lau, A. Y. A., Yeung, H. Y. E., Chik, S. W., Chiu, H. C., … Pile, J. (2013). A comparison of the post-storm recovery of two sandy beaches on Hong Kong Island, southern China. *Quaternary International*, *304*, 163–175. https://doi.org/10.1016/j.quaint.2013.04.002